Journal of Medicinal Chemistry

Subscriber access provided by University of Massachusetts Amherst Libraries

Article

Development of (E)-2-((1,4-dimethylpiperazin-2-ylidene)amino)-5-nitro-N-phenylbenzamide, ML336: novel 2-amidinophenylbenzamides as potent inhibitors of Venezuelan Equine Encephalitis Virus

Chad E. Schroeder, Tuanli Yao, Julie Sotsky, Robert A. Smith, Sudeshna Roy, Yong-Kyu Chu, Haixun Guo, Nichole A. Tower, James W. Noah, Sarah McKellip, Melinda Sosa, Lynn Rasmussen, Layton H. Smith, E. Lucile White, Jeffrey Aubé, Colleen B. Jonsson, Donghoon Chung, and Jennifer E. Golden

J. Med. Chem., **Just Accepted Manuscript** • DOI: 10.1021/jm501203v • Publication Date (Web): 22 Sep 2014

Downloaded from http://pubs.acs.org on September 28, 2014

Just Accepted

"Just Accepted" manuscripts have been peer-reviewed and accepted for publication. They are posted online prior to technical editing, formatting for publication and author proofing. The American Chemical Society provides "Just Accepted" as a free service to the research community to expedite the dissemination of scientific material as soon as possible after acceptance. "Just Accepted" manuscripts appear in full in PDF format accompanied by an HTML abstract. "Just Accepted" manuscripts have been fully peer reviewed, but should not be considered the official version of record. They are accessible to all readers and citable by the Digital Object Identifier (DOI®). "Just Accepted" is an optional service offered to authors. Therefore, the "Just Accepted" Web site may not include all articles that will be published in the journal. After a manuscript is technically edited and formatted, it will be removed from the "Just Accepted" Web site and published as an ASAP article. Note that technical editing may introduce minor changes to the manuscript text and/or graphics which could affect content, and all legal disclaimers and ethical guidelines that apply to the journal pertain. ACS cannot be held responsible for errors or consequences arising from the use of information contained in these "Just Accepted" manuscripts.

ACS Publications
High quality. High impact.

Journal of Medicinal Chemistry is published by the American Chemical Society. 1155 Sixteenth Street N.W., Washington, DC 20036

Published by American Chemical Society. Copyright © American Chemical Society. However, no copyright claim is made to original U.S. Government works, or works produced by employees of any Commonwealth realm Crown government in the course of their duties.

Development of (*E*)-2-((1,4-dimethylpiperazin-2-ylidene)amino)-5-nitro-*N*-phenylbenzamide, ML336: novel 2-amidinophenylbenzamides as potent inhibitors of Venezuelan Equine Encephalitis Virus

Chad E. Schroeder,[§] Tuanli Yao,[§] Julie Sotsky,[‡] Robert A. Smith,[§] Sudeshna Roy,[§] Yong-Kyu Chu,[‡] Haixun Guo,[‡] Nichole A. Tower,[ϕ] James W. Noah,[ϕ] Sara McKellip,[ϕ] Melinda Sosa,[ϕ] Lynn Rasmussen,[ϕ] Layton H. Smith,[†] E. Lucile White,[ϕ] Jeffrey Aubé,[§] Colleen B. Jonsson,[‡] Donghoon Chung,[‡] Jennifer E. Golden[§]*

[§]University of Kansas Specialized Chemistry Center, Lawrence, KS 66049

[‡]Department of Microbiology and Immunology and Center for Predictive Medicine for Biodefense and Emerging Infectious Diseases, University of Louisville, Louisville, KY 40202

[ϕ]Southern Research Institute, Birmingham, AL 35205

[†]*Conrad Prebys* Center for Chemical Genomics, Sanford-Burnham Medical Research Institute at Lake Nona, Orlando, FL, USA, 32827

[*]Corresponding author

ABSTRACT: Venezuelan equine encephalitis virus (VEEV) is an emerging pathogenic alphavirus that can cause significant disease in humans. Given the absence of therapeutic options available and the significance of VEEV as a weaponized agent, an optimization effort was initiated around a quinazolinone screening hit **1** with promising cellular antiviral activity (EC_{50} = 0.8 μM), limited cytotoxic liability (CC_{50} > 50 μM), and modest *in vitro* efficacy in reducing viral progeny (63-fold at 5 μM). Scaffold optimization revealed a novel rearrangement affording amidines, specifically compound **45**, which was found to potently inhibit several VEEV strains in the low nanomolar range without cytotoxicity, (EC_{50} = 0.02-0.04 μM, CC_{50} > 50 μM) while limiting *in vitro* viral replication (EC_{90} = 0.17 μM). Brain exposure was observed in mice with **45**, significant protection was observed in VEEV-infected mice at 5 mg/kg/day, and viral replication appeared to be inhibited through interference of viral non-structural proteins.

INTRODUCTION

Alphaviruses are a group of infectious pathogens found worldwide for which no therapeutic agents have been successfully developed. Approximately 30 alphaviruses of the *Togaviridae* family have been identified, and almost a third contribute significantly to human disease.[1] Most members of the alphavirus genus are transmitted by infected mosquitoes. Depending on the virus, infection generally manifests in one of two forms.[2] Arthritogenic alphaviruses such as Chikungunya, Ross River, Mayaro, and Sindbis viruses cause fever, rash, and persistent arthralgia. Eastern, Western, and Venezuelan equine encephalitis viruses (EEEV, WEEV and VEEV, respectively) are endemic to the American continent and produce a flu-like illness in human populations that is characterized by fever, headache, myalgia, sore throat, vomiting, and virus-dependent propensity to progress to fatal encephalitis.[3,4] Encephalitic

alphaviruses have garnered increased attention in recent years due to the ease with which they can be weaponized as biothreats.[5] For instance, VEEV was previously investigated as an incapacitating bioterror agent given that low levels of viral exposure caused illness and that the virus could be generated in high titer and stored indefinitely.[6,7] These features, combined with the discovery that the virus could be aerosolized, are responsible for VEEV, along with EEEV and WEEV, being classified as Centers for Disease Control (CDC) and National Institute for Allergy and Infectious Diseases (NIAID) category B bioterrorism agents.[8,9]

VEEV provides an attractive platform to investigate intervention of alphavirus infection. Virus is difficult to detect in blood and cerebral-spinal fluid (CSF) samples from patients infected with EEEV or WEEV; however, VEEV can be easily found in these and other biospecimens, thus facilitating the *in vivo* efficacy assessment of new antiviral agents.[10] Additionally, VEEV has a better safety margin than that of EEEV. While some strains of EEEV have a human mortality rate averaging 50%, fatality due to VEEV infection is rare (< 1% overall).[4,11] Nonetheless, VEEV is a serious pathogen that warrants specific attention in its own right. Fatality rates in equines can reach up to 85%, and in human populations, up to 14% of infected patients experience chronic neurological complications that manifest as depression, behavioral disorders, convulsions, and impairment of coordinated muscular movement.[12] Based on epidemiologic data, the neurological disease is more prevalent and severe in children based.[13]

While there are no FDA-approved human vaccines or therapeutics available for VEEV (or any alphavirus), advances in the development of agents targeting encephalitic alphaviruses are investigated and have recently been reviewed.[4] To date, human VEEV vaccines have seen limited success due to insufficient protection, transient immunity or the incidence of adverse reactions.[14-19] Several small molecule-derived anti-VEEV compounds have been reported,

though most have uncharacterized mechanisms of action, demonstrate only weak *in vitro* inhibition and do not appear to have been pursued further.[7,20-22] An exception includes the diazodiimine compound, BIOder, an inhibitor of the GSK-3β host protein that governs proinflammatory responses.[23] While this proof-of-concept compound showed only partial efficacy in preventing mice from succumbing to VEEV infection, it demonstrated the potential of using a small molecule inhibitor in this capacity. Given the health threat posed by alphaviruses and the absence of available countermeasures, a program aimed at identifying small molecule-derived VEEV inhibitors was undertaken by our team.

RESULTS AND DISCUSSION

Screening and Hit Identification. As part of the Molecular Libraries Probe Production Centers Network (MLPCN),[24] this team launched a screening campaign seeking new structural hits for development as potent, small molecule inhibitors of VEEV. The high throughput screen (HTS), a cell-based assay that measured the ability of a compound to inhibit a VEEV-induced cytopathic effect (CPE), was developed and validated employing TC-83 strain, an attenuated vaccine strain of wild type Trinidad donkey VEEV.[25,26,27] The use of the TC-83 strain was advantageous due to its high congruency to wild type virus, fewer regulatory restrictions in handling (BL-2 and non-select agent); however, it retained high similarity to wildtype with respect to genomic sequence, replication mechanism, and ability to obtain high viral titer (> 10e9 pfu/mL) compared to that observed with wild type virus.[26] A total of 348,140 compounds from the Molecular Libraries Small Molecule Repository (MLSMR) were evaluated at a single concentration of 20 μM, resulting in 3608 hits that inhibited a VEEV-induced CPE by > 14%. Of these, 90 compounds were identified through subsequent antiviral dose-response experiments and cellular cytotoxicity

(Vero 76 cells) evaluation that resulted in ≥ 30% inhibition, CPE EC_{50} ≤ 12.5 μM, and CC_{50} ≥ 25 μM, respectively. The hit list was further refined to five compounds based on lack of reactive functionality, synthetic feasibility, PubChem promiscuity[28] analysis, acceptable aqueous solubility in PBS buffer for the most promising scaffolds, and validation of activity from resynthesized and purified powder samples. Validated hits were further assessed in an *in vitro* viral titer reduction assay to quantitatively determine their effect on the production of infectious progeny virus. The team drafted a set of project criteria that, if reached, would afford a soluble, cellular-acting, small molecule probe that was efficacious in potently attenuating a VEEV-induced CPE and reduced viral plaques by at least 1000-fold at a concentration of 5 μM. These properties, coupled with a sufficient window for cytotoxicity and suitable physiochemical parameters, were expected to deliver an impactful probe compound worthy of *in vivo* efficacy studies. The quinazolinone chemotype, represented by hit compound **1**, was an attractive starting point due to its preliminary activity and physiochemical profile. Improvements were explored by tuning various structural components (shaded regions, Fig. 1).

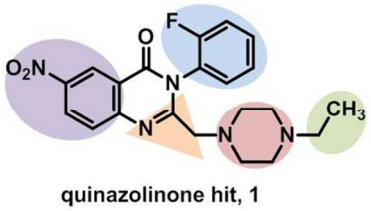

quinazolinone hit, 1

CPE EC_{50} = 0.8 μM
CC_{50} > 50 μM
titer reduction (5 μM) = 63-fold
molecular weight = 411.43 g/mol
cLogP = 3.4
tPSA = 90.96
PBS solubility = 122 μg/mL

Figure 1. Shaded regions of hit compound **1** optimized by structure-activity relationships.

Quinazolinone Chemistry and SAR. The optimization process was driven by the TC-83 CPE-based dose response assay, cytotoxicity assessment, and titer reduction experiments. The possibility of performing any future *in vivo* studies was expected to pivot on the ability of an anti-VEEV compound to reach encephalitic brain tissue.[29] As such, careful attention was paid to

balancing potency in both CPE-based and titer reduction assays with suitable physiochemical properties such as cLogP, polar surface area (tPSA), molecular weight, and solubility such that analogs were more likely to be CNS-permeable.[30,31] Generally, analogs of **1** were prepared in a three-step procedure that involved treating substituted anthranilic acids **2** with chloroacetyl chloride in the presence of triethylamine to afford 2-(2-chloroacetamido)-5-nitrobenzoic acid **3** (Scheme 1).[32] Dehydrative amidation was carried out by treating intermediates **3** with a selected aniline and $POCl_3$.[33] The resulting chloromethylquinazolinones **4** were aminated with alkylpiperazines to give quinazolinones **5**.[34]

Scheme 1. Synthetic Route for Assembly of Quinazolinone Analogs

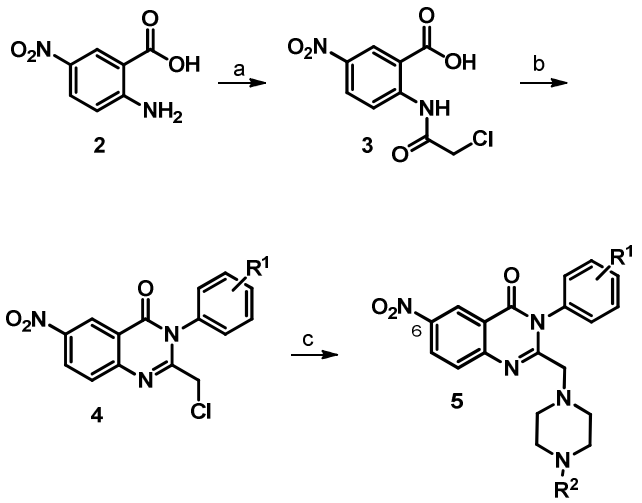

Reagents: a) $ClCOCH_2Cl$, NEt_3, CH_2Cl_2, 0 °C to rt, 95%; b) substituted aniline, $POCl_3$, acetonitrile, MWI, 150 °C, 56-70%; c) KI, K_2CO_3, alkylpiperazine, acetonitrile, MWI, 80 °C, 25-80%.

Survey of the scaffold began with determining the necessity of the C6-nitro functionality. Migration of the C6-nitro group to any other of the available C5-, C7-, or C8-positions afforded analogs without significant CPE assay potency (> 25 μM). Replacement of the nitro group was initially investigated on the parent scaffold bearing a 2-fluorophenyl moiety; however, once it

was determined that removal of the fluorine substituent from the phenyl group improved potency three-fold and substantially enhanced reduction in viral titer, subsequent generations of analogs were made with this alteration (Table 1, entries 1 vs. 4). Substitution of the nitro group with a hydrogen atom or a trifluoromethyl group resulted in loss of CPE assay activity (entries 2-3). Several replacements were studied, including a carboxylic acid, tetrazole, sulfonic acid, and amide isosteres; however, these changes were not tolerated with the exception of nitrile analog **10** (entry 6) which lost some potency and was inferior in reducing viral titer compared to hit compound **1**.

Table 1. Structure-Activity Relationships Involving the Quinazolinone C6-Nitro Group

entry	compound	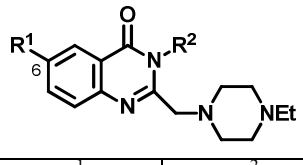		VEEV (TC-83) CPE (EC_{50}, μM)[a]	cytotoxicity (CC_{50}, μM)[b]	selectivity index (CC_{50}/EC_{50})	VEEV titer,[c,d] log reduction	cLogP[e]
		R^1	R^2					
1	**1**	NO_2	2-F-phenyl	0.8	> 50.0	> 62.5	1.8	3.4
2	**6**	H	2-F-phenyl	> 25.0	> 50.0	NA	NT	3.6
3	**7**	CF_3	2-F-phenyl	> 25.0	> 50.0	NA	NT	4.5
4	**8**	NO_2	phenyl	0.3	> 50.0	> 166.7	> 7.8	3.3
5	**9**	I	phenyl	17.1	> 50.0	> 2.9	0.3	4.6
6	**10**	CN	phenyl	1.1	> 50.0	> 45.5	1.7	2.9
7	**11**	SO_3H	phenyl	> 25.0	> 50.0	NA	NT	-1.6
8	**12**	CO_2H	phenyl	> 25.0	> 50.0	NA	NT	1.2
9	**13**	*NH*-tetrazole	phenyl	> 25.0	> 50.0	NA	NT	3.0
10	**14**	$CONH_2$	phenyl	> 25.0	> 50.0	NA	NT	2.4
11	**15**	$CONMe_2$	phenyl	> 25.0	> 50.0	NA	NT	2.2
12	**16**	2-pyridyl	phenyl	> 25.0	> 50.0	NA	NT	4.1
13	**17**	3-pyridyl	phenyl	> 25.0	> 50.0	NA	NT	3.9

[a]Data were an average of > 3 experiments; [b]Data were an average of >2 experiments; [c]NT = not tested; [d]Data were collected using 5 μM of compound, and data was analyzed using Microsoft Excel 2010; [e]Data were calculated using SYBYL 8.0, Tripos Associates, St. Louis MO, 2010.

Given the potency dependency on the presence of the C6 nitro functionality, a majority of the SAR was investigated with this moiety preserved, and attention shifted to modifications of the *N*-ethyl portion of the piperazine appendage (X-Y, Table 2). Replacement of the *N*-ethyl group for

N-methyl did not impact the CPE assay, but profoundly improved the reduction of viral plaques (entry 1). The introduction of a larger *N*-isopropyl substituent adversely affected potency, suggesting a spacial constraint in the binding site (entry 2). The loss of potency associated with the *N*-phenyl analog **20** also supported a steric argument; however, the observed effect may have been due, at least in part, to the preference of a more basic amine capable of having beneficial interactions with proximal binding residues. To address this ambiguity, *N*-H analog **21** was prepared and found to be superior to any of its predecessors in the study with respect to CPE potency (EC_{50} = 0.2 μM) and titer reduction efficacy (> 7.8 log). Furthermore, the analogs bearing non-basic, *N*-ethyl replacements (*e.g.*, morpholine **22**, piperidine **23**, and amide **24**) were determined to possess significantly inferior activity profiles compared to *N*-H analog **21**. These combined results suggested that there is a strong preference for a basic *N*-H moiety in this region of the scaffold.

In a parallel effort the effect of changing the 2-fluorophenyl amide substituent was also surveyed (Table 2, R^2). Compared to the hit **1**, a dramatic increase in titer reduction was observed by incorporating a 3-fluorophenyl group (**25**, entry 8); however, simplifying to a non-substituted phenyl ring advantageously produced analog **8** with similar overall activity to analog **21**. Exchange of the phenyl group for alkyl groups of various sizes or a hydrogen atom was not tolerated (**27-30**, entries 11-14). Other significant findings included the hybrid R^2-phenyl-containing, *N*-H piperazine **31** and 4-methoxyphenyl derivative **34** which both produced a favorable reduction in CPE and viral plaques that was comparable to analog **21**. Gratifyingly, this endeavor revealed that several analogs could be generated with improved activity as compared to the hit compound by modulating two distinct regions of the scaffold while advantageously adjusting molecular weight and cLogP.

Table 2. Quinazolinone Structure-Activity Relationships Involving the *N*-aryl and Piperazine Groups

entry	compound	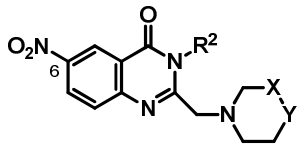			VEEV (TC-83) CPE (EC_{50}, μM)[a]	cytotoxicity (CC_{50}, μM)[b]	selectivity index (CC_{50}/ EC_{50})[c]	VEEV titer,[d,e] log reduction	cLogP[f]
		R^2	X	Y					
1	**18**	2-F-phenyl	CH_2	*N*-methyl	0.8	> 50.0	> 62.5	7.1	2.9
2	**19**	2-F-phenyl	CH_2	*N*-*i*-propyl	4.4	> 50.0	> 11.4	NT	3.7
3	**20**	2-F-phenyl	CH_2	*N*-phenyl	> 25.0	> 50.0	NA	NT	4.3
4	**21**	2-F-phenyl	CH_2	*N*-H	0.2	> 50.0	> 250.0	> 7.8	2.3
5	**22**	2-F-phenyl	CH_2	O	8.7	> 50.0	> 5.7	0.3	2.3
6	**23**	2-F-phenyl	CH_2	CH_2	4.7	> 50.0	> 10.6	0.4	3.6
7	**24**	2-F-phenyl	CO	*N*-H	> 25.0	> 50.0	NA	NT	2.0
8	**25**	3-F-phenyl	CH_2	*N*-ethyl	0.4	> 50.0	> 125.0	7.1	3.4
9	**26**	4-F-phenyl	CH_2	*N*-ethyl	0.8	> 50.0	> 62.5	5.9	3.4
10	**8**	phenyl	CH_2	*N*-ethyl	0.3	> 50.0	> 166.7	> 7.8	3.3
11	**27**	methyl	CH_2	*N*-ethyl	> 25.0	> 50.0	NA	NT	1.3
12	**28**	*i*-propyl	CH_2	*N*-ethyl	> 25.0	> 50.0	NA	NT	2.1
13	**29**	benzyl	CH_2	*N*-ethyl	> 25.0	> 50.0	NA	NT	3.0
14	**30**	H	CH_2	*N*-ethyl	> 25.0	> 50.0	NA	NT	1.5
15	**31**	phenyl	CH_2	*N*-H	0.2	> 50.0	> 250.0	> 7.8	2.1
16	**32**	2-MeO-phenyl	CH_2	*N*-H	> 25.0	> 50.0	NA	NT	2.2
17	**33**	3-MeO-phenyl	CH_2	*N*-H	5.1	> 50.0	9.8	NT	2.2
18	**34**	4-MeO-phenyl	CH_2	*N*-H	0.2	> 50.0	> 250	> 7.4	2.2
19	**35**	3-NMe_2-phenyl	CH_2	*N*-H	> 25.0	> 50.0	NA	NT	2.6
20	**36**	4-NMe_2-phenyl	CH_2	*N*-H	> 25.0	> 50.0	NA	NT	2.6
21	**37**	3-thiophene	CH_2	*N*-H	1.4	> 50.0	> 35.7	NT	1.8

[a]Data were an average of > 3 experiments; [b]Data were an average of >2 experiments;[c]NA = not applicable; [d]NT = not tested; [e]Data were collected using 5 μM of compound, and data was analyzed using Microsoft Excel 2010; [f]Data were calculated using SYBYL 8.0, Tripos Associates, St. Louis M, 2010.

More extensive study of the piperazine appendage included excision of the methylene linkage between the quinazolinone core to provide piperazine **38** and *NH*-piperidine analog **39** (Table 3), neither of which led to impressive CPE inhibition. Trading the piperazine group for a hexahydropyrimidine attachment or ring expanded 1,4-diazepane moiety only marginally affected CPE potency as compared to hit **1** (analogs **40** and **41**, respectively). Nonetheless, the team pursued a series of open-chain, diamino analogs that are represented by *n*-propylamine **42**.

Interestingly, **42** showed respectable CPE inhibition (EC_{50} = 0.6 μM), but it was the only one of its kind that was isolated.

Table 3. Quinazolinone Structure-Activity Relationships Involving the Alkylpiperazine Appendage

entry	compound	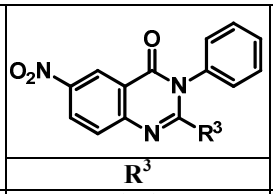 R^3	VEEV (TC-83) CPE (EC_{50}, μM)[a]	cytotoxicity (CC_{50}, μM)[b]	selectivity index (CC_{50}/EC_{50})	VEEV titer,[c,d] log reduction	cLogP[e]
1	**38**	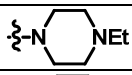	> 25.0	> 50.0	NA	NT	3.5
2	**39**	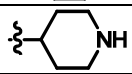	3.6	> 50.0	> 13.9	NT	3.6
3	**40**	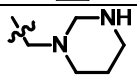	1.1	> 50.0	> 45.5	NT	2.2
4	**41**	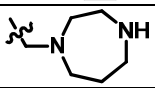	0.9	> 50.0	> 55.6	NT	2.1
5	**42**	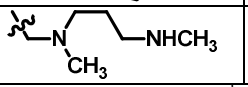	0.6	> 50.0	> 83.3	NT	2.4

[a]Data were an average of > 3 experiments; [b]Data are an average of >2 experiments; [c]NT = not tested; [d]Data were collected using 5 μM of compound, and data was analyzed using Microsoft Excel 2010; [e]Data were calculated using SYBYL 8.0, Tripos Associates, St. Louis M, 2010.

2-Amidinephenylbenzamide Chemistry. Examination of reactions employing a two carbon-tethered, acyclic diamine revealed the formation of a rearranged (*E*)-amidine **45** that was structurally confirmed by ^{1}H and ^{13}C NMR, NOESY, and 2D NMR spectroscopy (Scheme 2).[35] The reaction was initially carried out with mono-BOC protected diamines, thus providing a snapshot of the reaction pathway leading to the amidine product by proceeding through intermediate **44**; however, a one-pot conversion was achieved with symmetrically substituted diamines to afford **45** in a reasonable 69% yield. Amidines were the only isolated products from the reaction, and the exclusive isolation of the (*E*)-configured double bond amidine was presumed to result from electronic and steric contributions in the transition state. Interestingly,

amidines were generated when chloromethylquinolinone starting materials were treated with diamines separated by a two-carbon linkage, but a three-carbon tethered diamine produced the expected quinazolinone **42**. It is reasoned that amidine formation is favored when the reaction proceeds through a six-membered, spirocyclic intermediate such as **46**, resulting from an intramolecular attack of the terminal amine, followed by carbon-nitrogen bond cleavage. To our knowledge, this rearrangement has not been previously reported, and as such, a more comprehensive examination of the scope of this transformation is underway and will be disclosed in due course.[35]

Scheme 2. Formation of Rearranged Amidines

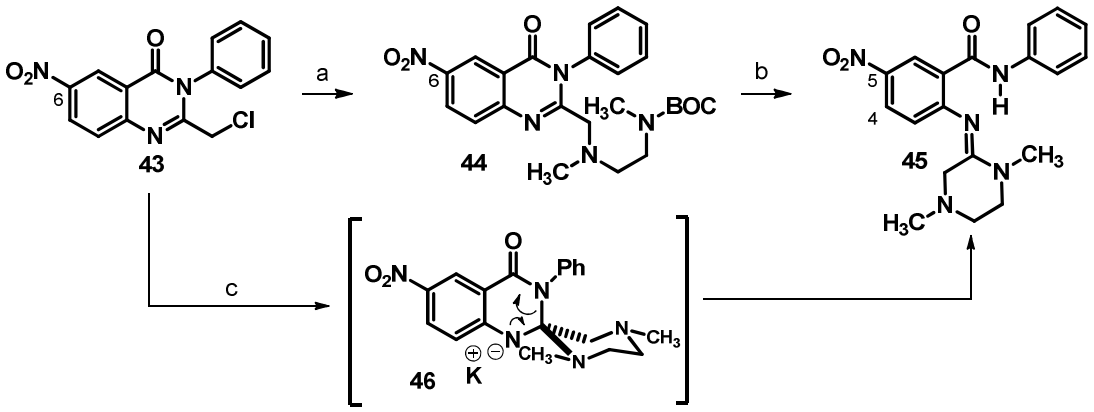

Reagents: (a) $CH_3NHCH_2CH_2NCH_3BOC$, KI, K_2CO_3, CH_3CN, MWI, 80 °C, 10 min, 35%; (b) TFA, CH_2Cl_2, rt, 45 min, then aq. $NaHCO_3$, 50%; (c) $CH_3NHCH_2CH_2NHCH_3$, K_2CO_3, CH_3CN, 50 °C, 2 h, 69%.

2-Amidinephenylbenzamide SAR. The conversion of quinazolinone intermediate **43** to amidine **45** represented a fortuitous scaffold modification, resulting in a nearly a 7-fold improvement in antiviral potency over the best quinazoline-based analogs while preserving the viral titer reduction capability and non-cytotoxic attributes (**45**, Table 4). Functional groups that were optimized for the quinazolinone scaffold showed a correlative enhancement of antiviral potency for the amidine series, though at an improved, low-nanomolar threshold. While the importance of

the quinazolinone C6-nitro group to retaining potency translated to the corresponding C5-position of the amidine chemotype, it was notable that the nitro group could be migrated to the amidine C4 position (compound **58**) or replaced with a fluorine atom or nitrile group (**60** and **63**, respectively) without obliterating activity.

Table 4. Amidine Structure-Activity Relationships

entry	compound	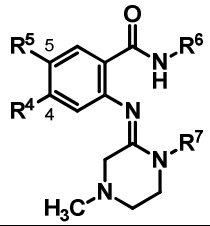				VEEV (TC-83) CPE potency[a]	cyto-toxicity[b]	selectivity index[c]	VEEV titer,[d,e]	cLogP[f]
		R^4	R^5	R^6	R^7	EC_{50}, μM	CC_{50}, μM	CC_{50}/EC_{50}	log reduction	
1	**45**	H	NO_2	phenyl	CH_3	0.03	> 50.0	> 1666.7	> 7.2	3.4
2	**47**	H	NO_2	phenyl	CH_2CH_3	0.05	> 50.0	> 1000.0	> 7.2	4.0
3	**48**	H	NO_2	3-thiophene	CH_3	0.5	> 50.0	100.0	NT	3.1
4	**49**	H	NO_2	2-CH_3O-phenyl	CH_3	33.7	> 50.0	> 1.5	NT	3.4
5	**50**	H	NO_2	3-CH_3O-phenyl	CH_3	8.1	> 50.0	> 6.2	NT	3.4
6	**51**	H	NO_2	4-CH_3O-phenyl	CH_3	0.04	> 50.0	> 1250.0	> 7.2	3.4
7	**52**	H	NO_2	2-F-phenyl	CH_3	0.2	> 50.0	> 250.0	> 3.8	3.6
8	**53**	H	NO_2	3-F-phenyl	CH_3	0.1	> 50.0	> 500.0	NT	3.6
9	**54**	H	NO_2	4-F-phenyl	CH_3	0.09	> 50.0	> 555.6	NT	3.6
10	**55**	H	NO_2	*i*-propyl	CH_3	> 25.0	> 50.0	NA	NT	2.8
11	**56**	H	NO_2	benzyl	CH_3	3.7	> 50.0	> 13.5	NT	3.8
12	**57**	H	H	phenyl	CH_3	> 25.0	> 50.0	NA	NT	3.3
13	**58**	NO_2	H	phenyl	CH_3	8.4	> 50.0	> 6.0	NT	3.4
14	**59**	F	H	phenyl	CH_3	> 25.0	> 50.0	NA	NT	3.6
15	**60**	H	F	phenyl	CH_3	6.4	> 50.0	> 7.8	NT	3.6
16	**61**	F	F	phenyl	CH_3	4.4	> 50.0	> 11.4	NT	3.8
17	**62**	H	CF_3	phenyl	CH_3	22.3	> 50.0	> 2.2	NT	4.5
18	**63**	H	CN	phenyl	CH_3	0.4	> 50.0	> 125.0	> 5.8	3.2
19	**64**	Cl	CN	phenyl	CH_3	0.1	> 50.0	> 500.0	NT	3.8

20	**65**	F	CN	phenyl	CH_3	0.4	> 50.0	> 125.0	NT	3.4
21	**66**	H	CN	2-F-phenyl	CH_3	3.7	> 50.0	> 13.5	NT	3.3
22	**67**	H	CN	3-F-phenyl	CH_3	0.8	> 50.0	> 62.5	> 1.4	3.3
23	**68**	H	CO_2CH_3	phenyl	CH_3	2.0	> 50.0	> 25.0	NT	3.6

[a]Data were an average of > 3 experiments; [b]Data were an average of > 2experiments;[c]NA = not applicable; [d]NT = not tested; [e]Data were collected using 5 μM of compound, and data was analyzed using Microsoft Excel 2010; [f]Data were calculated using SYBYL 8.0, Tripos Associates, St. Louis M, 2010.

The result of this effort revealed a set of amidine-derived VEEV inhibitors with exceptional, low nanomolar antiviral potency, a robust selectivity window and significant titer reduction efficacy. A subset of the most active representatives from the amidine series and the quinazolinone series (generally, those with CPE EC_{50} values ≤ 1 μM), were also evaluated in a CPE assay using wild type VEEV, Trinidad Donkey (TrD) strain, to confirm activity against a clinically relevant virus. Gratifyingly, strong agreement was observed across TC-83 and TrD strains for both chemotypes, especially for the most promising amidines of interest (entries 1-3, Table 5).

Table 5. Comparison of Cellular Data and Physiochemical Properties of Key Compounds

entry	**parameter**		**comparative data**		
	compound		**1**	**45**	**51**
1	CPE EC_{50}, TC-83 strain		0.8 μM	0.03 μM	0.04 μM
2	CPE EC_{50}, V3526 strain		0.3 μM	0.02 μM	0.02 μM
3	CPE EC_{50}, TrD strain		0.6 μM	0.04 μM	0.05 μM
4	titer reduction, TC-83 strain	5 μM compound concentration	1.8 log (69-fold)	7.2 log (16 million fold)	7.2 log (16 million fold)
5		1 μM compound concentration	0.5 log (3-fold)	7.2 log (16 million fold)	7.2 log (16 million fold)
6		0.5 μM compound concentration	NT	5.8 log (630,000 fold)	NT
7		dose response, EC_{90}	NT	0.17 μM	0.17 μM
8	titer reduction, TrD strain	5 μM compound concentration	no measurable viral replication	no measurable viral replication	no measurable viral replication
9		1 μM compound concentration	2.4 log (251-fold)	no measurable viral replication	no measurable viral replication
10		0.5 μM compound	NT	no measurable	no measurable

	concentration		viral replication	viral replication
11	Vero 76 cellular toxicity, CC_{50}	> 50.0 μM	> 50.0 μM	> 50.0 μM
12	aqueous solubility, PBS buffer	> 122.0 μg/mL	40.4 μg/mL	105.6 μg/mL
13	molecular weight[a]	411.4 g/mol	367.4 g/mol	397.4 g/mol
14	topological polar surface area, tPSA[a]	91.0 $Å^2$	99.8 $Å^2$	109.0 $Å^2$
15	cLogP[b]	3.4	3.4	3.4
16	hydrogen bond donors[c]	0	1	1
17	hydrogen bond acceptors[c]	7	5	6
18	heavy atoms[c]	30	27	29
19	ligand efficiency, LE	0.28	0.39	0.36
20	lipophilic ligand efficiency, LLE	2.7	4.1	4.1

NT = not tested; [a]Data were generated using CambridgeSoft ChemBioDraw, version 12. [b]Data were calculated using SYBYL 8.0, Tripos Associates, St. Louis M, 2010. [c]PubChem calculated chemical and physical parameters.

Pharmacology of Compound 45. Compared to the hit quinazolinone **1**, analogs **45** and **51** showed the best enhancement of CPE potency while also benefitting from decreased molecular weight and maintained cLogP. These compounds were also assessed in plaque reduction assays employing TC-83 or TrD strains at lower compound concentrations than the 5 μM concentration used during the SAR evaluation phase (entries 4-10, Table 5). While all three compounds blocked detectable levels of viral replication of wildtype TrD strain at 5 μM, only the amidines were effective at 0.5 μM, the lowest concentration tested initially. Assessment of compounds **45** and **51** in a dose response titer reduction assay revealed an EC_{90} = 0.17 μM for both compounds, demonstrating that in the 150 nM range, only 1/10 of virus was produced compared to the control, indicating efficient inhibition of virus replication. While rearrangement of the structural architecture from quinazolinones to amidines altered the number of hydrogen bond donors and acceptors, the cLogP values remained constant and improvements in ligand efficiency[36] and lipophilic ligand efficiency[37] were due to enhancements in potency alone. Analogs **45** and **51** were relatively evenly matched with respect to *in vitro* potency and efficacy; however, amidine **45** was slightly favored in terms of reduced molecular weight and topological polar surface area.

Consequently, amidine **45** was selected as the lead probe compound, ML336, and the compound was characterized further in terms of its *in vitro* pharmacology to establish a baseline profile against which future analogs could be optimized (Table 6). Diminished solubility was observed in CPE assay medium compared to an assessment in PBS, however, the solubility concentrations were still well above (~ 1200 to 3700-fold) the observed EC_{50} of the compound in the CPE assay (entries 1-2, table 6). The compound showed exceptional chemical stability in the presence of an excess of dithiotreitol (DTT). Aqueous stability, assessed initially in PBS, showed some liability, though this was shown to be an effect of some solubility limitation in that particular medium (entries 4-5, Table 6). In mice, compound **45** demonstrated limited liabilities in plasma stability and moderate plasma protein binding (entries 6-8). A parallel artificial membrane permeability assay (PAMPA) was used as an *in vitro* model of passive, transcellular blood-brain barrier (BBB) permeability at biological pH. Compound **45** registered at the lower end of the moderately permeable range of this assay.

Table 6. Summary of *In Vitro* Pharmacology Data for Compound 45 (ML336)

entry	assessment		result
1	aqueous solubility, 1x PBS, pH 7.4[a]		40.4 μg/mL, 110.0 μM
2	aqueous solubility, VEEV CPE assay medium[b]		13.1 μg/mL, or 35.7 μM
3	chemical stability with 5x DTT, 8 h[c]		99.0% parent remaining
4	aqueous stability, 48 h[c]	PBS, pH 7.4	82.9% parent remaining
5		1:1 PBS:acetonitrile	95.9% parent remaining
6	plasma stability, % remaining after 3 h (mouse)[a]		65.4% parent remaining
7	plasma protein binding, % bound[a]	1 μM (mouse)	85.0%
8		10 μM (mouse)	77.0%
9	BBB PAMPA, pH 7.4[a,d]		13 x 10^{-6} cm/s
10	hepatic microsomal stability, after 1 hour (mouse)[a]		42.9% parent remaining
11	hepatocyte toxicity (Fa2N-4), LD_{50} (human)[a]		> 25.0 μM
12	CYP450 inhibition profile, percent inhibition at 10 μM[a,e]	1A2 (human)	1.5 %
13		2C9 (human)	7 %
14		2C19 (human)	17 %

15		2D6 (human)	28 %
16		3A4 (human)	18 %
17	PanLabs profiling panel: assessment of percent inhibition of 67 host derived targets at a 10 μM compound concentration[f]		norepinephrine transporter, 91%

[a]Data collected by Ms. Arianna Mangravita-Novo at the *Conrad Prebys* Sanford Burnham Medical Research Institute; [b]CPE assay medium = high glucose DMEM with 10% FBS and 1x Pen/Strep; [c]Data collected by Mr. Patrick Porubsky at the University of Kansas Analytical Chemistry Core, Specialized Chemistry Center; [d]Donor and Acceptor pH: 7.4; Controls: Verapamil-HCl (highly permeable): 138; Corticosterone (moderately permeable): 14; Theophylline (poorly permeable): 0.32; [e]Control inhibitors: For CYP3A4, ketoconazole, 99% inhibition; for CYP2C9, sulfaphenazole, 96% inhibition; for CYP1A2, α-naphtoflavone, 84% inhibition; for CYP2C19, lansoprazole, 86% inhibition; for CYP2D6, quinidine, 88-98% inhibition; [f]Eurofins PanLabs data, all targets were assessed in duplicate and complete profile is included in the supplemental material.

Cytochrome P450 induction was not assessed; however, only insignificant inhibition of 1A2, 2C9, 2C19, 2D6, and 3A4 was observed (< 30% at 10 μM, entries 12-16). Some metabolic liability was detected after 1 hour exposure to mouse liver homogenates (~43% of **45** remained), though the compound showed no toxicity (> 25 μM LD_{50}) toward human hepatocytes. Lastly, compound **45** was evaluated in radioligand binding assays against a panel of 67 GPCRs, ion channels and transporters.[38] At a single concentration of 10 μM, 91% inhibition of the human norepinephrine transporter was observed; however, inhibition of all other targets in the collection was ≤ 36%.[39] Overall, this pharmacological profile obtained of compound **45** was encouraging in combination with the potency and toxicity data that the prototype compound may be useful in establishing baseline optimization parameters for *in vivo* assessment.

To that end, preliminary *in vivo* mouse pharmacokinetic (PK) data was collected for compound **45** in order to assess plasma and brain exposure relative to time and dose (Table 7).[40] The concentration of compound **45**, delivered by intraperitoneal (IP) administration, was determined in plasma at 20 and 120 minutes post-administration for each of three doses (1, 5 and

10 mg/kg) with 3 mice in each cohort. Additionally, the concentration of compound **45** in brain tissue was determined at the terminal endpoint (120 min) for each group. In accordance with the *in vitro* PK profile, the compound was readily depleted from circulation over the experimental window; however, significant exposure was observed for each dose in plasma and brain tissue. Moreover, > 10-fold concentrations over the *in vitro* CPE assay EC_{50} values were observed in both plasma and brain for the 5 mg/kg and 10 mg/kg doses after 120 min.

Table 7. *In Vivo* Exposure Data for Compound 45 in Mice

compound **45** dose[a]	time (min)[b]	number of mice per group[c]	plasma data (mouse)		brain data (mouse)	
			average[d] concentration ± standard deviation (μM)	CV (%)	average[d] concentration ± standard deviation (μM)	CV (%)
1 mg/kg	20	3	0.20 ± 0.03	15.1	ND	ND
	120	3	0.023 ± 0.007	30.8	0.19 ± 0.22	115.8
5 mg/kg	20	3	1.45 ± 0.26	17.6	ND	ND
	120	3	0.29 ± 0.01	4.7	0.21± 0.02	10.7
10 mg/kg	20	3	2.68 ± 0.36	13.5	ND	ND
	120	3	0.49 ± 0.25	49.9	0.35 ± 0.06	17.0

[a]IP administration; [b]Each time point is an average of 2 LC/MC injections (< 20% difference); [c]C57BL/6 mice were used; [d]Data was an average of three independent experiments for each dose and timepoint (*i.e.*, 3 mice in each cohort, including vehicle control – not shown); CV = coefficient of variation; ND = not determined.

These preliminary *in vivo* studies encouraged us to evaluate **45** in a lethal mouse model of VEEV infection.[20] Single and multiple dose range finding studies were performed to define any potential toxicity of compound **45** in mice prior to conducting efficacy studies. The compound was administered IP twice daily to C3H/HeN mice in doses of 5 mg/kg/day and 40 mg/kg/day for four days. For all mice, no apparent toxicity or adverse effects were observed in the mice as measured by body weight loss, lethargy, hunched posture and ruffled fur. To test the *in vivo* efficacy of compound **45** in a 21-day lethal mouse model, compound **45** was administered IP at

2.5 mg/kg twice daily for four days to one group of VEEV (TC-83)-infected mice (Fig. 2).[41] Mice receiving treatment were dosed with compound four hours prior to intranasal exposure to VEEV TC-83. Compared to the infected, untreated group, significant survival rates (71%) were observed with VEEV-infected mice treated with compound **45**.

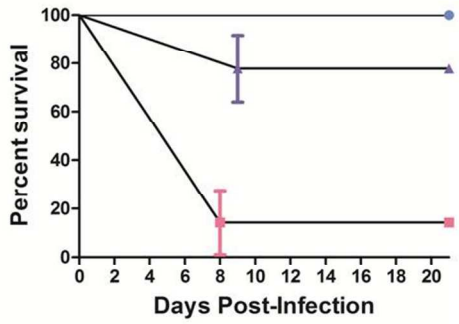

key	group description	# mice per group	# live mice at day 21	percent survival
●	vehicle (no virus or compound treatment)	7	7	100%
■	untreated VEEV infected mice	7	1	14%
▲	VEEV infected mice treated with **45** (5 mg/kg/day for 4 days)	7	5	71%

Figure 2. Survival data for VEEV infected C3H/HeN mice treated with compound **45** over a 21 day study compared to controls. Survival curves were generated using the Kaplan-Meier method[42] and were compared using the Log-rank (Mantel-Cox) Test; X^2 value = 11.70, p-value = 0.0029 (2 degrees of freedom). The error bars show the standard error of the mean.

Mechanism of Action Studies. To understand the regions of the viral protein that are important to the molecular action of the compound, an assay using hit quinazolinone **1**-resistant mutant viruses was performed. Previously we have reported the isolation of mutant virus strains that are resistant to hit quinazolinone **1** with mutations of Y102C and D116N in non-structural protein 2.[27] More recently, using the same method, we have isolated additional quinazolinone **1**-resistant mutant VEEV TC-83 strains with a mutation of Q120K in nsP4 (Table 8). The alphavirus genome comprises two open reading frames, a structural and non-structural segment. The structural segment encodes for proteins constituting the virion: (1) envelope proteins E1 and E2,

and (2) core nucleocapsid protein C. The nonstructural segment encodes non-structural proteins 1-4 (nsP1–nsP4) which are necessary for transcription and replication of viral RNA.[43]

Mutant viruses obtained from those studies[44] were used to examine the resistance profile of amidine **45**. To confirm that each of these sites conferred resistance, the amino acids were changed in VEEV V3526 by site-directed mutagenesis, and the EC_{50} value for compound **45** was measured for each mutant virus (Table 8). The activity of compound **45** significantly decreased when it was tested against these mutant viruses compared to the parental VEEV strains, suggesting that compound **45** may target a critical function of nsp2/nsp4 in the VEEV replicase complex, resulting in inhibition of viral RNA synthesis. At this point in time, a function has not been ascribed to the domain in the nsP2 or nsP4 that compound **45** targets, but more advanced experiments are underway to elucidate their role in the potent inhibition exhibited by these compounds.

Table 8. Effect of Compound 45 on Wildtype and Mutant VEE Viruses

VEEV strain	protein segment of located mutation	mutation	compound **45** CPE potency EC_{50} (μM)	fold loss of potency (mutant EC_{50}/parental EC_{50})
TC-83	nsP2	none (parental strain)	0.03	-
	nsP2	Y102C	17	567
	nsP2	D116N	19	633
	nsP4	Q210K	> 50	> 1667
V3526	nsP2	none (parental strain)	0.05	-
	nsP2	Y102C	19	380
	nsP4	Q210K	66	1320

CONCLUSION

With the emergence of alphavirus infections and the biohazards associated with their misuse has evolved an urgent need for effective countermeasures that have yet to be realized. Our efforts, directed at the identification and development of VEEV inhibitors, revealed a quinazolinone hit scaffold that was optimized through structural modification to afford novel, rearranged amidines with tremendous potential for further lead development and utility in dissecting novel mechanistic elements associated with alphavirus replication. The probe compound **45** showed potent inhibition of viral CPE for several strains of VEEV in the low nanomolar range without inducing cytotoxicity. These antiviral effects translated to impressive cellular efficacy in plaque reduction assays at submicromolar concentrations of compound, thus demonstrating the ability of amidine **45** to potently arrest viral replication. Gratifyingly, *in vitro* phamacokinetic data collected on amidine **45** predicted moderate brain exposure which was corroborated by preliminary pharmacokinetic studies in mice. These results helped to establish a dosing strategy for efficacy studies in which amidine **45** was shown to impart significant protection to VEEV-infected mice in a 21-day study. Mechanistically, these compounds appear to inhibit viral replication through a unique pathway involving interference with viral non-structural proteins 2 and 4. Ultimately, the discovery of amidine **45** and its analogs represent an exciting advance in alphavirus research in that these agents offer a distinctive mechanistic intervention and a potential therapeutic and biodefense opportunity for VEEV. Future work centers on optimizing the structural amidine architecture to refine *in vivo* pharmacokinetic parameters, evaluating these and improved compounds in advanced animal efficacy models for VEEV, determining specific proteins of mechanistic relevance, and profiling these compounds against other viruses of therapeutic interest.

EXPERIMENTAL SECTION

Chemistry. Purity of all final compounds was confirmed by HPLC/MS analyis and determined to be ≥ 95%. ^{1}H and ^{13}C NMR spectra were recorded on a Bruker AM 400 spectrometer (operating at 400 and 101 MHz respectively) or a Bruker AVIII spectrometer (operating at 500 and 126 MHz respectively) in $CDCl_3$ (residual internal standard $CHCl_3$ = δ 7.26), DMSO-d_6 (residual internal standard CD_3SOCD_2H = δ 2.50), or acetone-d_6 (residual internal standard CD_3COCD_2H = δ 2.05). The chemical shifts (δ) reported are given in parts per million (ppm) and the coupling constants (*J*) are in Hertz (Hz). The spin multiplicities are reported as s = singlet, br s = broad singlet, d = doublet, t = triplet, q = quartet, p = pentuplet, dd = doublet of doublet, dt = doublet of triplet, td = triplet of doublet, tt = triplet of triplet, and m = multiplet. The LC-MS analysis was performed on an Agilent 1200 RRL HPLC system with photodiode array UV detection and an Agilent 6224 TOF mass spectrometer. The chromatographic method utilized the following parameters: a Waters Acquity BEH C-18 2.1 x 50 mm, 1.7 μm column; UV detection wavelength = 214 nm; flow rate = 0.4 mL/min; gradient = 5-100% MeCN over 3 minutes with a hold of 0.8 minutes at 100% MeCN; the aqueous mobile phase contained 0.15% NH_4OH. The mass spectrometer utilized the following parameters: an Agilent multimode source which simultaneously acquires ESI+/APCI+; a reference mass solution consisting of purine and hexakis(1*H*, 1*H*, 3*H*-tetrafluoropropoxy) phosphazine; and a make-up solvent of 90:10:0.1 $MeOH/H_2O/HCO_2H$ which was introduced to the LC flow prior to the source to assist ionization. Melting points were determined on a Stanford Research Systems OptiMelt apparatus. Microwave irradiated reactions were carried out using a Biotage Initiator Classic synthesizer. Flash chromatography separations were carried out using a Teledyne Isco CombiFlash Rf 200 purification system with silica gel columns. Mass-directed fractionation separations were carried

out using an Agilent 1200 HPLC system with photodiode array UV detection and an Agilent 6120 mass spectrometer. The chromatographic method utilized a Waters XBridge C-18, 19 x 150 mm, 5 μm column; UV detection wavelength = 214 nm; flow rate = 20 mL/min; focused gradient = 5-100% MeCN; the aqueous mobile phase contained 0.15% NH_4OH. Quinazolinones were generally prepared according to Scheme 1 and by the protocols detailed for compound **1**, below, unless otherwise specified. Amidines were prepared by either of two methods depicted in Scheme 2 and by the protocols detailed for compound **45**, below, unless otherwise specified.

Synthesis of 2-((4-Ethylpiperazin-1-yl)methyl)-3-(2-fluorophenyl)-6-nitroquinazolin-4(3*H*)-one (1). *Step 1, Synthesis of 2-(2-chloroacetamido)-5-nitrobenzoic acid (**3**).* Triethylamine (2 mL, 14.4 mmol) was added to a solution of 2-amino-5-nitro-benzoic acid (2.280 g, 12.5 mmol) in dry CH_2Cl_2 (34 mL) under an atmosphere of nitrogen. The mixture was lowered to 0 °C and a solution of chloroacetyl chloride (1.09 mL, 13.7 mmol) in dry CH_2Cl_2 (16 mL) was slowly added. The mixture was allowed to reach rt over 2 h. The solvent was removed *in vacuo* and water (20 mL) was added. The product was filtered, rinsed with water (2 x 20 mL), and then rinsed with 5% ether/hexanes (3 x 30 mL) to give **3** (3.08 g, 95%) as a light-brown solid. ^{1}H NMR (400 MHz, acetone-d_6) δ 12.26 (s, 1H), 8.93–8.87 (m, 2H), 8.45 (dd, J = 9.3, 2.8 Hz, 1H), 4.42 (s, 2H). ^{13}C NMR (101 MHz, acetone-d_6) δ 168.5, 166.9, 146.8, 143.1, 129.9, 127.7, 121.0, 117.2, 44.1.

Step 2: Synthesis of 2-(chloromethyl)-3-(2-fluorophenyl)-6-nitroquinazolin-4(3H)-one. A MW vial was charged with 2-(2-chloroacetamido)-5-nitrobenzoic acid (1.93 g, 7.5 mmol) and capped. The atmosphere was evacuated under reduced pressure and flushed with Ar. Dry MeCN (14 mL) was added to the vial, followed by $POCl_3$ (1.5 mL, 16.1 mmol) and a solution of 2-fluoroaniline (0.97 mL, 10.1 mmol) in dry MeCN (4 mL). The mixture was heated in a MW reactor at 150 °C

for 15 min. The mixture was transferred to a larger flask and slowly quenched with saturated aq. $NaHCO_3$ (80 mL). The resulting solid was filtered and rinsed with water (3 x 50 mL) to give 2-(chloromethyl)-3-(2-fluorophenyl)-6-nitroquinazolin-4(3H)-one (1.39 g, 56%) as a burnt-orange solid. ^{1}H NMR (400 MHz, $CDCl_3$) δ 9.14 (d, *J* = 2.5 Hz, 1H), 8.60 (dd, *J* = 8.9, 2.6 Hz, 1H), 7.92 (d, *J* = 8.9 Hz, 1H), 7.64–7.57 (m, 1H), 7.48–7.31 (m, 3H), 4.40 (d, *J* = 12.0 Hz, 1H), 4.23 (d, *J* = 12.0 Hz, 1H).

*Step 3: Synthesis of 2-((4-ethylpiperazin-1-yl)methyl)-3-(2-fluorophenyl)-6-nitroquinazolin-4(3H)-one (**1**).* To a microwave vial, 2-(chloromethyl)-3-(2-fluorophenyl)-6-nitroquinazolin-4(3*H*)-one (560 mg, 1.7 mmol) was added and dissolved in dry MeCN (9 mL). Potassium carbonate (464 mg, 3.4 mmol), *N*-ethylpiperazine (0.30 mL, 2.4 mmol), and KI (106 mg, 0.64 mmol) were successively added, and the vial was capped. The mixture was heated in a MW reactor at 80 °C for 10 min. The mixture was concentrated and the product was purified by flash chromatography (0-10% MeOH/CH_2Cl_2) to give **1** (333 mg, 48%) as a pale-orange solid. ^{1}H NMR (400 MHz, $CDCl_3$) δ 9.15 (d, *J* = 2.6 Hz, 1H), 8.58 (dd, *J* = 8.9, 2.7 Hz, 1H), 7.88 (d, *J* = 8.9 Hz, 1H), 7.55–7.49 (m, 1H), 7.37–7.28 (m, 3H), 3.44 (d, *J* = 13.7 Hz, 1H), 3.27 (d, *J* = 13.7 Hz, 1H), 2.44–2.16 (m, 10H), 1.04 (t, *J* = 7.2 Hz, 3H). ^{13}C NMR (101 MHz, $CDCl_3$) δ 160.8, 159.4, 157.1, 156.9, 151.1, 146.2, 131.7, 131.6, 129.8, 129.4, 128.9, 124.7, 124.6, 124.4, 124.3, 123.9, 121.5, 116.8, 116.6, 61.8, 53.1, 52.6, 52.3, 12.1. LC-MS: ^{t}R = 3.18 min, purity = 98%. HRMS (*m*/*z*): calcd for $C_{21}H_{23}FN_5O_3$ $(M + H)^+$ 412.1779; found 412.1808.

2-((4-Ethylpiperazin-1-yl)methyl)-6-nitro-3-phenylquinazolin-4(3*H*)-one (8). Following the same three step procedure used to synthesize **1**, 2-(chloromethyl)-6-nitro-3-phenylquinazolin-4(3*H*)-one (168 mg, 0.53 mmol) was used to produce **8** (101 mg, 48%) as a pale-yellow solid. mp 179-182 °C (decomp.). ^{1}H NMR (400 MHz, $CDCl_3$) δ 9.11 (d, *J* = 2.6 Hz, 1H), 8.55 (dd, *J* =

9.0, 2.6 Hz, 1H), 7.87 (d, *J* = 9.0 Hz, 1H), 7.58–7.50 (m, 3H), 7.34–7.29 (m, 2H), 3.27 (s, 2H), 2.48–2.26 (m, 10H), 1.06 (t, *J* = 7.2 Hz, 3H). ^{13}C NMR (101 MHz, $CDCl_3$) δ 161.5, 157.1, 151.2, 146.0, 136.1, 129.7, 129.5, 129.3, 128.8, 128.6, 123.8, 121.6, 61.3, 53.0, 52.7, 52.4, 12.0. LC-MS: ^{t}R = 2.90 min, purity = 98%. HRMS (*m*/*z*): calcd for $C_{21}H_{24}N_5O_3$ $(M + H)^+$ 394.1874; found 394.1896.

2-((4-Ethylpiperazin-1-yl)methyl)-4-oxo-3-phenyl-3,4-dihydroquinazoline-6-carbonitrile (10). Following the same procedure used to synthesize **1**, 2-(chloromethyl)-4-oxo-3-phenyl-3,4-dihydroquinazoline-6-carbonitrile (25 mg, 0.085 mmol) was used to produce **10** (20 mg, 63%) as a yellow solid. mp 136-142 °C (decomp.). ^{1}H NMR (400 MHz, $CDCl_3$) δ 8.59 (d, *J* = 2.0 Hz, 1H), 7.95 (dd, *J* = 8.5, 2.0 Hz, 1H), 7.83 (d, *J* = 8.5 Hz, 1H), 7.59–7.46 (m, 3H), 7.34–7.27 (m, 2H), 3.26 (s, 2H), 2.56–2.22 (m, 10H), 1.06 (t, *J* = 7.2 Hz, 3H). ^{13}C NMR (126 MHz, $CDCl_3$) δ 161.2, 156.5, 149.7, 136.5, 136.1, 132.6, 129.7, 129.6, 129.0, 128.8, 121.9, 118.1, 110.7, 61.2, 52.7, 52.6, 52.4, 11.8. LC-MS: ^{t}R = 2.91 min, purity = 97%. HRMS (*m*/*z*): calcd for $C_{22}H_{24}N_5O$ $(M + H)^+$ 374.1975; found 374.1996.

3-(2-Fluorophenyl)-2-((4-methylpiperazin-1-yl)methyl)-6-nitroquinazolin-4(3*H*)-one (18). Following the same procedure used to synthesize **1** (except the reaction was heated at 150 °C for 15 min), 2-(chloromethyl)-3-(2-fluorophenyl)-6-nitroquinazolin-4(3*H*)-one (83 mg, 0.25 mmol) and 1-methyl piperazine (0.04 mL, 0.36 mmol) were used to produce **18** (31 mg, 31%) as a light-orange solid. mp 218-221 °C. ^{1}H NMR (400 MHz, $CDCl_3$) δ 9.11 (d, *J* = 2.6 Hz, 1H), 8.55 (dd, *J* = 8.9, 2.6 Hz, 1H), 7.86 (d, *J* = 8.9 Hz, 1H), 7.55–7.47 (m, 1H), 7.36–7.24 (m, 3H), 3.42 (d, *J* = 13.7 Hz, 1H), 3.25 (d, *J* = 13.7 Hz, 1H), 2.38–2.18 (m, 11H). ^{13}C NMR (101 MHz, $CDCl_3$) δ 160.7, 159.4, 157.0, 156.9, 151.1, 146.1, 131.6, 131.6, 129.7, 129.3, 128.8, 124.7, 124.6, 124.4,

124.2, 123.8, 121.4, 116.7, 116.5, 61.7, 54.9, 53.0, 46.1. LC-MS: ^{t}R = 2.20 min, purity = 96%. HRMS (*m*/*z*): calcd for $C_{20}H_{21}FN_5O_3$ $(M + H)^+$ 398.1623; found 398.1654.

3-(2-Fluorophenyl)-6-nitro-2-(piperazin-1-ylmethyl)quinazolin-4(3*H*)-one (21). *Step 1, synthesis of tert-butyl-4-((3-(2-fluorophenyl)-6-nitro-4-oxo-3,4-dihydroquinazolin-2-yl)methyl)piperazine-1-carboxylate.* In a round-bottom flask, 2-(chloromethyl)-3-(2-fluorophenyl)-6-nitroquinazolin-4(3*H*)-one (250 mg, 0.75 mmol) was dissolved in dry MeCN (3.5 mL) under a nitrogen atmosphere. Potassium carbonate (124 mg, 0.90 mmol), 1-BOC-piperazine (279 mg, 1.50 mmol), and KI (87 mg, 0.52 mmol) were added to the flask and the mixture was thermally heated at 80 °C for 4 hours. The solvent was removed *in vacuo* and water (10 mL) was added. The product was extracted with EtOAc (3 x 10 mL), washed with saturated aq. NH_4Cl (10 mL) and saturated aq. $NaHCO_3$ (10 mL), and then dried with Na_2SO_4. The product was purified by flash chromatography (0-50% EtOAc/hexanes) to give the title compound (201 mg, 56%) as a white solid. ^{1}H NMR (400 MHz, $CDCl_3$) δ 9.09–9.04 (m, 1H), 8.51 (dd, *J* = 8.9, 2.7 Hz, 1H), 7.83–7.77 (m, 1H), 7.50–7.42 (m, 1H), 7.29–7.20 (m, 3H), 3.39 (d, *J* = 13.7 Hz, 1H), 3.24–3.09 (m, 5H), 2.25–2.16 (m, 2H), 2.11–2.02 (m, 2H), 1.36 (s, 9H).

*Step 2, synthesis of 3-(2-fluorophenyl)-6-nitro-2-(piperazin-1-ylmethyl)quinazolin-4(3H)-one (**21**).* In a round-bottom flask, *tert*-butyl 4-((3-(2-fluorophenyl)-6-nitro-4-oxo-3,4-dihydroquinazolin-2-yl)methyl)piperazine-1-carboxylate (71 mg, 0.15 mmol) was dissolved in dry CH_2Cl_2 (2 mL) and TFA (0.07 mL, 0.91 mmol) was slowly added dropwise. The reaction mixture was stirred at rt for 2 hours, then diluted with water (4 mL) and CH_2Cl_2 (4 mL). The reaction was quenched to pH 10 using saturated aq. Na_2CO_3 (1 mL). The product was extracted with CH_2Cl_2 (3 x 10 mL), dried with Na_2SO_4 and purified by flash chromatography (0-10% MeOH/CH_2Cl_2) to give **21** (25 mg, 44%) as a white solid. mp 202-204 °C (decomp.). ^{1}H NMR

(400 MHz, $CDCl_3$) δ 9.15 (d, *J* = 2.0 Hz, 1H), 8.64–8.53 (m, 1H), 7.89 (d, *J* = 8.8 Hz, 1H), 7.59–7.49 (m, 1H), 7.41–7.25 (m, 3H), 3.52–3.37 (m, 2H), 3.27 (d, *J* = 13.6 Hz, 1H), 2.81–2.59 (m, 4H), 2.37–2.10 (m, 4H). ^{13}C NMR (101 MHz, $CDCl_3$) δ 160.7, 159.4, 157.0, 156.9, 151.1, 146.1, 131.7, 131.6, 129.7, 129.3, 128.8, 124.7, 124.6, 124.4, 124.3, 123.8, 121.4, 116.7, 116.5, 62.4, 54.3, 45.8. LC-MS: ^{t}R = 2.22 min, purity = 100%. HRMS (*m*/*z*): calcd for $C_{19}H_{19}FN_5O_3$ $(M + H)^+$ 384.1466; found 384.1471.

2-((4-Ethylpiperazin-1-yl)methyl)-3-(3-fluorophenyl)-6-nitroquinazolin-4(3*H*)-one (25). Following the same procedure used to synthesize **1**, 2-(chloromethyl)-3-(3-fluorophenyl)-6-nitroquinazolin-4(3*H*)-one (157 mg, 0.47 mmol) was used to produce **25** (155 mg, 80%) as a white solid, mp 187-190 °C (decomp.). ^{1}H NMR (400 MHz, $CDCl_3$) δ 9.10 (d, *J* = 2.6 Hz, 1H), 8.56 (dd, *J* = 9.0, 2.6 Hz, 1H), 7.89 (d, *J* = 9.0 Hz, 1H), 7.58–7.50 (m, 1H), 7.29–7.22 (m, 1H), 7.18–7.12 (m, 2H), 3.36–3.26 (m, 2H), 2.51–2.24 (m, 10H), 1.07 (t, *J* = 7.2 Hz, 3H). ^{13}C NMR (101 MHz, $CDCl_3$) δ 164.0, 161.6, 161.3, 156.6, 151.0, 146.1, 137.3, 137.2, 130.6, 130.5, 129.4, 128.8, 124.6, 124.6, 123.7, 121.5, 117.2, 117.0, 116.9, 116.7, 61.4, 53.1, 52.7, 52.3, 12.0. LC-MS: ^{t}R = 2.93 min, purity = 98%. HRMS (*m*/*z*): calcd for $C_{21}H_{23}FN_5O_3$ $(M + H)^+$ 412.1779; found 412.1808.

2-((4-Ethylpiperazin-1-yl)methyl)-3-(4-fluorophenyl)-6-nitroquinazolin-4(3*H*)-one (26). Following the same procedure used to synthesize **1**, 2-(chloromethyl)-3-(4-fluorophenyl)-6-nitroquinazolin-4(3*H*)-one (169 mg, 0.51 mmol) was used to produce **26** as a white solid (160 mg, 77%), mp 196-199 °C (decomp.). ^{1}H NMR (400 MHz, $CDCl_3$) δ 9.10 (d, *J* = 2.6 Hz, 1H), 8.56 (dd, *J* = 9.0, 2.6 Hz, 1H), 7.88 (d, *J* = 8.9 Hz, 1H), 7.37–7.31 (m, 2H), 7.28–7.21 (m, 2H), 3.29 (s, 2H), 2.52–2.24 (m, 10H), 1.07 (t, *J* = 7.2 Hz, 3H). ^{13}C NMR (101 MHz, $CDCl_3$) δ 164.2, 161.7, 161.6, 156.9, 151.0, 146.0, 131.9, 131.8, 130.9, 130.8, 129.3, 128.7, 123.7, 121.5, 116.5,

116.3, 61.5, 53.1, 52.8, 52.3, 12.1. LC-MS: ^{t}R = 2.98 min, purity = 98%. HRMS (*m*/*z*): calcd for $C_{21}H_{23}FN_5O_3$ $(M + H)^+$ 412.1779; found 412.1802.

6-Nitro-3-phenyl-2-(piperazin-1-ylmethyl)quinazolin-4(3*H*)-one (31). Following the same procedure used to synthesize **21**, compound **31** was obtained as a white solid (49 mg, 86%), mp 190-195 °C. ^{1}H NMR (400 MHz, DMSO-d_6) δ 8.82 (d, *J* = 2.5 Hz, 1H), 8.61 (dd, *J* = 9.0, 2.7 Hz, 1H), 7.93 (d, *J* = 9.0 Hz, 1H), 7.58–7.49 (m, 5H), 3.25 (s, 2H), 2.70–2.62 (m, 4H), 2.23–2.15 (m, 4H). ^{13}C NMR (126 MHz, $CDCl_3$) δ 161.6, 157.0, 151.2, 146.0, 136.1, 129.7, 129.5, 129.3, 128.8, 128.7, 123.9, 121.6, 62.0, 54.2, 45.9. LC-MS: ^{t}R = 2.61 min, purity = 99%. HRMS (*m*/*z*): calcd for $C_{19}H_{20}N_5O_3$ $(M + H)^+$ 366.1561; found 366.1567.

3-(4-Methoxyphenyl)-6-nitro-2-(piperazin-1-ylmethyl)quinazolin-4(3*H*)-one (34). Following the same procedure used to synthesize **21**, compound **34** was obtained as a white solid (146 mg, 90%), mp 180-183 °C (decomp.). ^{1}H NMR (500 MHz, DMSO-d_6) δ 8.80 (d, *J* = 2.5 Hz, 1H), 8.59 (dd, *J* = 9.0, 2.7 Hz, 1H), 7.92 (d, *J* = 9.0 Hz, 1H), 7.41–7.37 (m, 2H), 7.10–7.06 (m, 2H), 3.82 (s, 3H), 3.20 (s, 2H), 2.58–2.52 (m, 4H), 2.16–2.10 (m, 4H). ^{13}C NMR (126 MHz, DMSO-d_6) δ 161.2, 159.3, 157.9, 150.9, 145.2, 130.2, 129.1, 128.8, 128.5, 122.5, 121.2, 113.9, 61.7, 55.5, 53.5, 45.2. LC-MS: ^{t}R = 2.73 min, purity = 99%. HRMS (*m*/*z*): calcd for $C_{20}H_{22}N_5O_4$ $(M + H)^+$ 396.1666; found 396.1670.

6-Nitro-2-(piperazin-1-ylmethyl)-3-(thiophen-3-yl)quinazolin-4(3*H*)-one (37). Following the same procedure used to synthesize **21** except during purification 5% NH_4OH was added to MeOH in the mobile phase, **37** was obtained as a white solid (79 mg, 58%), mp 205-208 °C (decomp.). ^{1}H NMR (400 MHz, $CDCl_3$) δ 9.12 (d, *J* = 2.6 Hz, 1H), 8.55 (dd, *J* = 8.9, 2.6 Hz, 1H), 7.86 (d, *J* = 8.9 Hz, 1H), 7.49 (dd, *J* = 5.1, 3.2 Hz, 1H), 7.42 (dd, *J* = 3.2, 1.3 Hz, 1H), 7.09

(dd, J = 5.1, 1.3 Hz, 1H), 3.33 (br s, 2H), 2.86–2.75 (m, 4H), 2.42–2.31 (m, 4H). ^{13}C NMR (101 MHz, $CDCl_3$) δ 161.4, 157.2, 150.8, 145.9, 133.3, 129.2, 128.6, 127.0, 125.8, 123.7, 123.5, 121.3, 62.0, 54.5, 46.0. LC-MS: ^{t}R = 2.62 min, purity = 100%. HRMS (*m*/*z*): calcd for $C_{17}H_{18}N_5O_3S$ $(M + H)^+$ 372.1125; found 372.1138.

2-(4-Ethylpiperazin-1-yl)-6-nitro-3-phenylquinazolin-4(3*H*)-one (38). *Step 1, synthesis of 6-nitro-3-phenylquinazoline-2,4(1H,3H)-dione.* To a stirred mixture of 2-amino-5-nitrobenzanilide (1.97 g, 7.66 mmol) in dry toluene (25 mL) was carefully added a solution of 20% (w/v) phosgene in toluene (15 mL, 30.3 mmol). ***CAUTION!*** *Phosgene is highly toxic and should be handled with care*. The mixture was heated at 95 °C for 19.5 h, then concentrated and purified by flash column chromatography (0–90% EtOAc/hexanes) to give the title compound (1.45 g, 67%) as a colorless solid. mp 297–299 °C (decomp.). ^{1}H NMR (400 MHz, acetone-d_6) δ 10.93 (s, 1H), 8.82 (d, J = 2.6 Hz, 1H), 8.53 (dd, J = 9.0, 2.6 Hz, 1H), 7.58–7.45 (m, 4H), 7.45–7.39 (m, 2H).

Step 2, synthesis of 2-(4-ethylpiperazin-1-yl)-6-nitro-3-phenylquinazolin-4(3H)-one (38). Phosphorus pentachloride (44 mg, 0.21 mmol), 6-nitro-3-phenylquinazoline-2,4(1*H*,3*H*)-dione (44 mg, 0.16 mmol), and phosphorus oxychloride (1.5 mL, 16 mmol) were heated in a sealed vial at 120 °C for 16 hours. The mixture was concentrated and redissolved in dry CH_2Cl_2 (5 mL). *N*-ethylpiperazine (142 mg, 1.24 mmol) was added and the mixture was briefly stirred at rt. The mixture was re-concentrated and the product was purified by mass-directed fractionation to give **38** (19 mg, 31%) as a yellow solid. mp 179–182 °C (decomp.). ^{1}H NMR (400 MHz, DMSO-d_6) δ 8.71 (d, J = 2.6 Hz, 1H), 8.46 (dd, J = 9.0, 2.8 Hz, 1H), 7.61–7.44 (m, 6H), 3.24–3.13 (m, 4H), 2.26–2.16 (m, 2H), 2.16–2.05 (m, 4H), 0.92 (t, J = 7.1 Hz, 3H). ^{13}C NMR (101 MHz, DMSO-d_6) δ 161.6, 156.0, 152.6, 142.4, 137.1, 128.9, 128.7, 128.6, 128.4, 126.7, 123.1, 117.9, 51.3, 51.2,

48.2, 11.7. LC-MS: ^{t}R = 3.29 min, purity = 100%. HRMS (*m*/*z*): calcd for $C_{20}H_{22}N_5O_3$ $(M + H)^+$ 380.1717; found 380.1732.

6-Nitro-3-phenyl-2-(piperidin-4-yl)quinazolin-4(3*H*)-one (39). *Step 1, synthesis of tert-butyl 4-((4-nitro-2-(phenylcarbamoyl)phenyl)carbamoyl)piperidine-1-carboxylate.* To a stirred mixture of 1-(*tert*-butoxycarbonyl)piperidine-4-carboxylic acid (213 mg, 0.93 mmol) in dry CH_2Cl_2 (10 mL) was added a catalytic amount of DMF (2 drops) at rt followed by the dropwise addition of oxalyl chloride (479 mg, 3.77 mmol). The mixture was stirred at rt for 2 hours and concentrated. The remaining residue was redissolved in dry THF (5 mL) and MeCN (5 mL) and slowly added to a mixture of 2-amino-5-nitro-*N*-phenylbenzamide (211 mg, 0.82 mmol) and 95% (w/w) NaH (128 mg, 5.07 mmol) in dry THF (10 mL) at -78 °C. The mixture was allowed to warm to rt and stirred for 16 hours. The reaction was quenched with water, extracted with EtOAc (3x), washed with brine, and dried with Na_2SO_4. The product was purified by reverse-phase chromatography (C-18, 10-100% MeCN/H_2O) to give the title compound (38 mg, 10%) as an off-white solid. ^{1}H NMR (400 MHz, acetone-d_6) δ 11.41 (s, 1H), 10.17 (s, 1H), 8.84 (d, J = 9.3 Hz, 1H), 8.73 (d, J = 2.6 Hz, 1H), 8.35 (dd, J = 9.3, 2.7 Hz, 1H), 7.77–7.71 (m, 2H), 7.38 (tt, J = 7.6, 2.0 Hz, 2H), 7.18 (tt, J = 7.1, 1.1 Hz, 1H), 4.08 (d, J = 12.7 Hz, 2H), 2.91–2.72 (m, 2H), 2.63 (tt, J = 11.5, 3.8 Hz, 1H), 1.97–1.88 (m, 2H), 1.67–1.53 (m, 2H), 1.40 (s, 9H).

*Step 2, synthesis of 6-nitro-3-phenyl-2-(piperidin-4-yl)quinazolin-4(3H)-one (**39**).* Triethylamine (10 mg, 0.10 mmol), chlorotrimethylsilane (9 mg, 0.08 mmol), and *tert*-butyl-4-((4-nitro-2-(phenylcarbamoyl)phenyl)carbamoyl)piperidine-1-carboxylate (38 mg, 0.08 mmol) were dissolved in dry MeCN (1.5 mL) and heated in a MW reactor at 150 °C for 10 min. The mixture was purified by flash chromatography (0-60% EtOAc/hexanes) and re-dissolved in 3:1 CH_2Cl_2/TFA (2 mL). The reaction mixture was stirred at rt for 16 hours and concentrated. The

product was purified by mass-directed fractionation to give **39** (14.4 mg, 51%) as a yellow solid. mp 193–200 °C (decomp.). ^{1}H NMR (400 MHz, DMSO-d_6) δ 8.80 (d, J = 2.5 Hz, 1H), 8.59 (dd, J = 9.0, 2.7 Hz, 1H), 7.89 (d, J = 9.0 Hz, 1H), 7.65–7.49 (m, 6H), 2.90 (d, J = 10.6 Hz, 2H), 2.41–2.26 (m, 1H), 2.19–2.02 (m, 2H), 1.81–1.62 (m, 4H). ^{13}C NMR (101 MHz, DMSO-d_6) δ 160.8, 151.5, 144.7, 136.6, 129.6, 129.4, 128.7, 128.5, 128.4, 122.4, 120.6, 45.5, 41.5, 30.8. LC-MS: ^{t}R = 2.96 min, purity = 100%. HRMS (*m*/*z*): calcd for $C_{19}H_{19}N_4O_3$ $(M + H)^+$ 351.1452; found 351.1460.

2-((Methyl(3-(methylamino)propyl)amino)methyl)-6-nitro-3-phenylquinazolin-4(3*H*)-one, 2,2,2-trifluoroacetic acid salt (42). *Step 1, synthesis of tert-butyl-methyl(3-(methyl((6-nitro-4-oxo-3-phenyl-3,4-dihydroquinazolin-2-yl)methyl)amino)propyl)carbamate.* Following the same procedure used to synthesize **1**, 2-(chloromethyl)-6-nitro-3-phenylquinazolin-4(3*H*)-one (221 mg, 0.70 mmol) and *tert*-butyl methyl(3-(methylamino)propyl)carbamate (240 mg, 1.19 mmol) were used to produce the title compound (106 mg, 31%) as a pale-orange solid. ^{1}H NMR (400 MHz, $CDCl_3$) δ 9.08 (d, J = 2.6 Hz, 1H), 8.54 (dd, J = 9.0, 2.7 Hz, 1H), 7.89 (d, J = 8.9 Hz, 1H), 7.61–7.51 (m, 3H), 7.33–7.28 (m, 2H), 3.31 (s, 2H), 3.13–3.05 (m, 2H), 2.78 (s, 3H), 2.32–2.25 (m, 2H), 2.17 (s, 3H), 1.50 (p, J = 7.3 Hz, 2H), 1.42 (s, 9H).

*Step 2, synthesis of 2-((methyl(3-(methylamino)propyl)amino)methyl)-6-nitro-3-phenylquinazolin-4(3H)-one, 2,2,2-trifluoroacetic acid salt (**42**).* In a round-bottom flask, *tert*-butyl methyl(3-(methyl((6-nitro-4-oxo-3-phenyl-3,4-dihydroquinazolin-2-yl)methyl)amino)propyl)carbamate (148 mg, 0.31 mmol) was dissolved in dry CH_2Cl_2 (5 mL) and TFA (2 mL, 26.1 mmol) was added dropwise. The reaction mixture was stirred at rt for 45 min, then diluted with water (10 mL) and CH_2Cl_2 (10 mL). The mixture was adjusted to pH 10 using saturated aq. Na_2CO_3 (10 mL). The layers were separated and the aq. layer was extracted

with CH_2Cl_2 (3 x 25 mL). The combined organic extracts were dried with Na_2SO_4. The product was purified through a reverse-phase, C-18 column (5-100% MeCN/H_2O, RediSep Rf Gold C18 column from Teledyne Isco) to give **42** (11 mg, 7%) as a white solid. ^{1}H NMR (500 MHz, $CDCl_3$) δ 10.51 (br s, 2H), 9.10 (d, *J* = 2.6 Hz, 1H), 8.56 (dd, *J* = 9.0, 2.7 Hz, 1H), 7.84 (d, *J* = 9.0 Hz, 1H), 7.66–7.54 (m, 3H), 7.37–7.32 (m, 2H), 3.39–3.33 (m, 2H), 3.25–3.19 (m, 2H), 2.79 (s, 3H), 2.71 (t, *J* = 5.6 Hz, 2H), 2.36 (s, 3H), 1.96 (p, *J* = 5.5 Hz, 2H). ^{13}C NMR (126 MHz, $CDCl_3$) δ 162.8, 162.6, 162.3, 162.0, 160.7, 157.7, 150.8, 145.9, 135.1, 130.5, 130.2, 129.0, 128.2, 128.0, 123.9, 121.3, 120.2, 117.9, 115.6, 113.2, 59.6, 56.9, 50.4, 43.3, 33.0, 21.9. LC-MS: ^{t}R = 2.25 min, purity = 97%. HRMS (*m*/*z*): calcd for $C_{20}H_{24}N_5O_3$ $(M + H)^+$ 382.1874; found 382.1878.

(*E*)-2-((1,4-Dimethylpiperazin-2-ylidene)amino)-5-nitro-*N*-phenylbenzamide (45). *Method A. Step 1, synthesis of tert-butyl-methyl(2-(methyl((6-nitro-4-oxo-3-phenyl-3,4-dihydroquinazolin-2-yl)methyl)amino)ethyl)carbamate (**44**).* To a MW vial, 2-(chloromethyl)-6-nitro-3-phenylquinazolin-4(3*H*)-one **43** (1.400 g, 4.4 mmol) was added and dissolved in dry MeCN (18 mL). Potassium carbonate (1.226 g, 8.9 mmol), *tert*-butyl-methyl(2-(methylamino)ethyl)carbamate (1.176 g, 6.3 mmol), and KI (0.280 g, 1.7 mmol) were successively added and the vial was capped. The mixture was heated in a MW reactor at 80 °C for 5 min. The mixture was concentrated and the product was purified by flash chromatography (0-10% MeOH/CH_2Cl_2, followed by 0-80% EtOAc/hexanes) to give *tert*-butyl-methyl(2-(methyl((6-nitro-4-oxo-3-phenyl-3,4-dihydroquinazolin-2-yl)methyl)amino)ethyl)carbamate **44** (0.719 g, 35%) as a pale-orange solid. ^{1}H NMR (400 MHz, $CDCl_3$) δ 9.13 (d, *J* = 2.6 Hz, 1H), 8.56 (dd, *J* = 9.0, 2.7 Hz, 1H), 7.89 (d, *J* = 9.0 Hz, 1H), 7.60–7.52 (m, 3H), 7.32–7.27 (m, 2H), 3.36 (s, 2H), 3.22–3.06 (m, 2H), 2.75 (br s, 3H), 2.48 (br s, 2H), 2.20 (s, 3H), 1.39 (s, 9H).

*Step 2, synthesis of (E)-2-((1,4-dimethylpiperazin-2-ylidene)amino)-5-nitro-N-phenylbenzamide (**45**).* To a stirred solution of tert-butyl-methyl(2-(methyl((6-nitro-4-oxo-3-phenyl-3,4-dihydroquinazolin-2-yl)methyl)amino)ethyl)carbamate **44** (678 mg, 1.45 mmol) in dry CH_2Cl_2 (20 mL), TFA (9.5 mL, 124 mmol) was slowly added. The reaction mixture was stirred at rt for 45 min, then diluted with water (40 mL) and CH_2Cl_2 (40 mL). The reaction was quenched to pH 10 using saturated aq. Na_2CO_3 (40 mL). The org. phase was separated and the aq. phase was extracted with CH_2Cl_2 (2 x 40 mL). The combined org. phase was concentrated and purified by flash chromatography (0-5% MeOH/CH_2Cl_2) to give **45** (265 mg, 50%) as a pale-yellow solid. mp 168-173 °C. ^{1}H NMR (500 MHz, $CDCl_3$) δ 10.99 (s, 1H), 9.15 (d, *J* = 2.8 Hz, 1H), 8.15 (dd, *J* = 8.8, 2.8 Hz, 1H), 7.65–7.60 (m, 2H), 7.38–7.33 (m, 2H), 7.12 (tt, *J* = 7.3, 1.2 Hz, 1H), 6.80 (d, *J* = 8.8 Hz, 1H), 3.47 (t, *J* = 5.7 Hz, 2H), 3.28 (s, 3H), 3.13 (s, 2H), 2.69 (t, *J* = 5.7 Hz, 2H), 2.26 (s, 3H). ^{13}C NMR (126 MHz, $CDCl_3$) δ 162.6, 156.4, 154.0, 142.8, 138.2, 129.1, 127.6, 126.4, 126.2, 124.2, 123.8, 120.2, 55.1, 51.8, 49.7, 45.3, 36.9. LC-MS: ^{t}R = 3.19 min, purity = 99%. HRMS (*m*/*z*): calcd for $C_{19}H_{22}N_5O_3$ $(M + H)^+$ 368.1717; found 368.1718.

(*E*)-2-((1,4-Dimethylpiperazin-2-ylidene)amino)-5-nitro-*N*-phenylbenzamide (45). *Method B.* To a stirred solution of 2-(chloromethyl)-6-nitro-3-phenylquinazolin-4(3*H*)-one (158 mg, 0.50 mmol) in dry MeCN (2 mL) was added K_2CO_3 (140 mg, 1.01 mmol) and *N*,*N*′-dimethylethylenediamine (0.08 mL, 0.74 mmol). The mixture was stirred at 50 °C for 2 hours. The mixture was concentrated and the product was purified by flash chromatography (0-5% MeOH/EtOAc) to give **45** (126 mg, 69%) as a yellow-orange solid. Analytical data was consistent with data obtained from Method A. LC-MS purity = 100%.

(*E*)-2-((1-Ethyl-4-methylpiperazin-2-ylidene)amino)-5-nitro-*N*-phenylbenzamide (47). Method A as given for **45**. Pale-yellow solid (18 mg, 26%), mp 150-157 °C (decomp.). ^{1}H NMR

(400 MHz, $CDCl_3$) δ 10.66 (s, 1H), 9.14 (d, *J* = 2.8 Hz, 1H), 8.16 (dd, *J* = 8.8, 2.8 Hz, 1H), 7.65–7.56 (m, 2H), 7.38–7.33 (m, 2H), 7.16–7.10 (m, 1H), 6.81 (d, *J* = 8.8 Hz, 1H), 3.78 (q, *J* = 7.1 Hz, 2H), 3.46 (t, *J* = 5.6 Hz, 2H), 3.12 (s, 2H), 2.68 (t, *J* = 5.6 Hz, 2H), 2.25 (s, 3H), 1.30 (t, *J* = 7.2 Hz, 3H). ^{13}C NMR (101 MHz, $CDCl_3$) δ 162.9, 155.9, 154.6, 142.9, 138.2, 129.2, 127.8, 126.6, 126.1, 124.5, 124.0, 120.7, 55.4, 52.0, 46.8, 45.3, 43.6, 12.2. LC-MS: ^{t}R = 3.34 min, purity = 99.7%. HRMS (*m*/*z*): calcd for $C_{20}H_{24}N_5O_3$ $(M + H)^+$ 382.1874; found 382.1894.

(*E*)-2-((1,4-Dimethylpiperazin-2-ylidene)amino)-5-nitro-*N*-(thiophen-3-yl)benzamide (48). Method B as given for **45**. Tan solid (46 mg, 50%), mp 170-175 °C (decomp.). ^{1}H NMR (400 MHz, $CDCl_3$) δ 11.26 (s, 1H), 9.16 (d, *J* = 2.8 Hz, 1H), 8.16 (dd, *J* = 8.8, 2.8 Hz, 1H), 7.75 (dd, *J* = 3.2, 1.3 Hz, 1H), 7.28–7.25 (m, 1H), 7.02 (dd, *J* = 5.2, 1.4 Hz, 1H), 6.80 (d, *J* = 8.7 Hz, 1H), 3.47 (t, *J* = 5.6 Hz, 2H), 3.28 (s, 3H), 3.13 (s, 2H), 2.69 (t, *J* = 5.7 Hz, 2H), 2.26 (s, 3H). ^{13}C NMR (101 MHz, $CDCl_3$) δ 162.1, 156.7, 153.9, 143.0, 135.9, 127.7, 126.4, 125.9, 124.7, 123.8, 121.1, 110.7, 55.2, 52.0, 49.8, 45.4, 36.9. LC-MS: ^{t}R = 3.19 min, purity = 99%. HRMS (*m*/*z*): calcd for $C_{17}H_{20}N_5O_3S$ $(M + H)^+$ 374.1281; found 374.1289.

(*E*)-2-((1,4-Dimethylpiperazin-2-ylidene)amino)-*N*-(4-methoxyphenyl)-5-nitrobenzamide (51). Method A as given for **45**. Yellow solid (33 mg, 41%). ^{1}H NMR (400 MHz, $CDCl_3$) δ 10.90 (s, 1H), 9.14 (d, *J* = 2.8 Hz, 1H), 8.14 (dd, *J* = 8.7, 2.8 Hz, 1H), 7.56–7.51 (m, 2H), 6.92–6.87 (m, 2H), 6.79 (d, *J* = 8.8 Hz, 1H), 3.80 (s, 3H), 3.47 (t, *J* = 5.6 Hz, 2H), 3.26 (s, 3H), 3.14 (s, 2H), 2.69 (t, *J* = 5.6 Hz, 2H), 2.26 (s, 3H). ^{13}C NMR (101 MHz, $CDCl_3$) δ 162.5, 156.5, 156.4, 154.0, 142.9, 131.5, 127.6, 126.34, 126.29, 123.8, 121.8, 114.3, 55.6, 55.2, 51.9, 49.8, 45.4, 37.0. LC-MS: ^{t}R = 3.17 min, purity = 99%. HRMS (*m*/*z*): calcd for $C_{20}H_{24}N_5O_4$ $(M + H)^+$ 398.1823; found 398.1840.

(*E*)-2-((1,4-Dimethylpiperazin-2-ylidene)amino)-*N*-(2-fluorophenyl)-5-nitrobenzamide (52). Method A as given for **45**. Yellow solid (71 mg, 89%). ^{1}H NMR (400 MHz, $CDCl_3$) δ 11.07 (s, 1H), 9.17 (d, *J* = 2.8 Hz, 1H), 8.53 (td, *J* = 8.1, 1.5 Hz, 1H), 8.14 (dd, *J* = 8.8, 2.8 Hz, 1H), 7.19–7.13 (m, 1H), 7.11–7.01 (m, 2H), 6.78 (d, *J* = 8.8 Hz, 1H), 3.46 (t, *J* = 5.6 Hz, 2H), 3.22 (d, *J* = 1.4 Hz, 3H), 3.14 (s, 2H), 2.68 (t, *J* = 5.7 Hz, 2H), 2.25 (s, 3H). ^{13}C NMR (101 MHz, $CDCl_3$) δ 163.0, 156.9, 154.8, 154.1, 151.7, 142.6, 128.0, 126.8, 126.7, 125.5, 124.8, 124.7, 124.34, 124.26, 124.0, 122.74, 122.72, 114.9, 114.7, 55.3, 51.9, 49.6, 45.3, 36.9, 36.8. LC-MS: ^{t}R = 3.37 min, purity = 99%. HRMS (*m*/*z*): calcd for $C_{19}H_{21}FN_5O_3$ $(M + H)^+$ 386.1623; found 386.1639.

(*E*)-2-((1,4-Dimethylpiperazin-2-ylidene)amino)-*N*-(3-fluorophenyl)-5-nitrobenzamide (53). Method A as given for **45**. Pale-yellow solid (12 mg, 39%), mp 165-169 °C (decomp.). ^{1}H NMR (400 MHz, $CDCl_3$) δ 11.06 (s, 1H), 9.14 (d, *J* = 2.8 Hz, 1H), 8.18 (dd, *J* = 8.8, 2.8 Hz, 1H), 7.57 (dt, *J* = 11.0, 2.3 Hz, 1H), 7.33–7.23 (m, 2H), 6.87–6.75 (m, 2H), 3.48 (t, *J* = 5.6 Hz, 2H), 3.29 (s, 3H), 3.13 (s, 2H), 2.69 (t, *J* = 5.7 Hz, 2H), 2.26 (s, 3H). ^{13}C NMR (126 MHz, $CDCl_3$) δ 164.2, 163.0, 162.3, 156.7, 154.0, 143.1, 139.94, 139.85, 130.3, 130.2, 127.9, 126.7, 126.1, 123.9, 115.53, 115.50, 111.1, 111.0, 107.9, 107.7, 55.3, 52.0, 49.9, 45.5, 37.1. LC-MS: ^{t}R = 3.33 min, purity = 97%. HRMS (*m*/*z*): calcd for $C_{19}H_{21}FN_5O_3$ $(M + H)^+$ 386.1623; found 386.1630.

(*E*)-2-((1,4-Dimethylpiperazin-2-ylidene)amino)-*N*-(4-fluorophenyl)-5-nitrobenzamide (54). Method A as given for **45**. Yellow solid (14 mg, 44%), mp 170-174 °C (decomp.). ^{1}H NMR (400 MHz, $CDCl_3$) δ 11.00 (s, 1H), 9.12 (d, *J* = 2.8 Hz, 1H), 8.14 (dd, *J* = 8.8, 2.8 Hz, 1H), 7.61–7.53 (m, 2H), 7.08–6.99 (m, 2H), 6.79 (d, *J* = 8.8 Hz, 1H), 3.47 (t, *J* = 5.6 Hz, 2H), 3.25 (s, 3H), 3.14 (s, 2H), 2.69 (t, *J* = 5.7 Hz, 2H), 2.26 (s, 3H). ^{13}C NMR (101 MHz, $CDCl_3$) δ 162.8, 160.6, 158.2, 156.7, 154.0, 143.0, 134.40, 134.38, 127.7, 126.5, 126.1, 123.8, 122.0, 121.9, 116.0,

115.7, 55.3, 52.0, 49.8, 45.4, 37.0. LC-MS: ^{t}R = 3.12 min, purity = 99%. HRMS (*m*/*z*): calcd for $C_{19}H_{21}FN_5O_3$ $(M + H)^+$ 386.1623; found 386.1631.

(*E*)-5-Cyano-2-((1,4-dimethylpiperazin-2-ylidene)amino)-*N*-phenylbenzamide (63). Method B as given for **45**. Yellow solid (25 mg, 71%), mp 167-169 °C. ^{1}H NMR (400 MHz, $CDCl_3$) δ 10.90 (s, 1H), 8.08 (dd, *J* = 11.8, 9.3 Hz, 1H), 7.61–7.51 (m, 3H), 7.37–7.30 (m, 2H), 7.13–7.07 (m, 1H), 6.53 (dd, *J* = 11.2, 6.9 Hz, 1H), 3.40 (t, *J* = 5.6 Hz, 2H), 3.22 (s, 3H), 3.07 (s, 2H), 2.64 (t, *J* = 5.6 Hz, 2H), 2.25 (s, 3H). ^{13}C NMR (101 MHz, $CDCl_3$) δ 163.0, 156.4, 152.2, 138.4, 136.2, 134.6, 129.2, 126.8, 124.3, 124.2, 120.4, 119.1, 106.0, 55.2, 52.0, 49.8, 45.5, 36.9. LC-MS: ^{t}R = 3.11 min, purity = 99.5%. HRMS (*m*/*z*): calcd for $C_{20}H_{22}N_5O$ $(M + H)^+$ 348.1819; found 348.1820.

(*E*)-4-Chloro-5-cyano-2-((1,4-dimethylpiperazin-2-ylidene)amino)-*N*-phenylbenzamide (64). Method B as given for **45**. Yellow solid (37 mg, 97%), mp 167-171 °C (decomp.). ^{1}H NMR (400 MHz, $CDCl_3$) δ 10.80 (s, 1H), 8.57 (s, 1H), 7.61–7.56 (m, 2H), 7.38–7.32 (m, 2H), 7.15–7.10 (m, 1H), 6.84 (s, 1H), 3.46 (t, *J* = 5.6 Hz, 2H), 3.26 (s, 3H), 3.13 (s, 2H), 2.69 (t, *J* = 5.6 Hz, 2H), 2.29 (s, 3H). ^{13}C NMR (101 MHz, $CDCl_3$) δ 162.2, 156.8, 152.8, 138.9, 138.2, 137.8, 129.2, 125.3, 124.5, 124.2, 120.4, 116.3, 106.6, 55.1, 51.9, 49.8, 45.4, 37.0. LC-MS: ^{t}R = 3.34 min, purity = 97%. HRMS (*m*/*z*): calcd for $C_{20}H_{21}ClN_5O$ $(M + H)^+$ 382.1429; found 382.1450.

(*E*)-Methyl 4-((1,4-dimethylpiperazin-2-ylidene)amino)-3-(phenylcarbamoyl)benzoate (68). *Step 1, synthesis of 2-(2-Chloroacetamido)-5-iodobenzoic acid.* Following the same procedure for **3**, 2-amino-5-iodobenzoic acid (6.58 g, 25.0 mmol) afforded the title compound (8.47 g, 100%) as a lavender solid. ^{1}H NMR (400 MHz, acetone-d_6) δ 11.86 (br s, 1H), 8.54 (d, *J* = 8.9 Hz, 1H), 8.41 (d, *J* = 2.2 Hz, 1H), 7.97 (dd, *J* = 8.9, 2.2 Hz, 1H), 4.35 (s, 2H).

Step 2, synthesis of 2-(chloromethyl)-6-iodo-3-phenylquinazolin-4(3H)-one. Procedure as done for **1**, step 2. White solid (0.95 g, 41%). ^{1}H NMR (400 MHz, $CDCl_3$) δ 8.62 (d, *J* = 1.9 Hz, 1H), 8.08 (dd, *J* = 8.6, 2.1 Hz, 1H), 7.62–7.55 (m, 3H), 7.51 (d, *J* = 8.6 Hz, 1H), 7.37–7.32 (m, 2H), 4.24 (s, 2H).

Step 3, synthesis of tert-butyl-(2-(((6-iodo-4-oxo-3-phenyl-3,4-dihydroquinazolin-2-yl)methyl)(methyl)amino)ethyl)(methyl)carbamate. Method A as given for **45**. Yellow oil (0.434 g, 90%). ^{1}H NMR (400 MHz, $CDCl_3$) δ 8.61 (d, *J* = 1.9 Hz, 1H), 8.04 (dd, *J* = 8.6, 2.1 Hz, 1H), 7.57–7.46 (m, 4H), 7.29–7.26 (m, 2H), 3.28 (s, 2H), 3.19–3.03 (m, 2H), 2.77–2.67 (m, 3H), 2.43 (br s, 2H), 2.15 (s, 3H), 1.38 (s, 9H).

Step 4, synthesis of methyl-2-(((2-((tert-butoxycarbonyl)(methyl)amino)ethyl)(methyl)amino)methyl)-4-oxo-3-phenyl-3,4-dihydroquinazoline-6-carboxylate. To a solution of *tert*-butyl-(2-(((6-iodo-4-oxo-3-phenyl-3,4-dihydroquinazolin-2-yl)methyl)(methyl)amino)ethyl)(methyl)carbamate (0.434 g, 0.79 mmol) in MeCN (4.4 mL) and MeOH (2.2 mL) were added $Pd(OAc)_2$ (18 mg, 0.08 mmol), DPPF (44 mg, 0.08 mmol), Et_3N (0.11 mL, 0.79 mmol) and K_2CO_3 (0.328 g, 2.37 mmol). The reaction mixture was purged with CO for 5 min, followed by stirring under 1 atm of CO (balloon) at 60 °C for 3 hours. The reaction mixture was filtered through Celite® and rinsed with EtOAc (2 x 10 mL). The filtrate was concentrated and purified by flash chromatography (EtOAc/hexanes). The title compound (0.248 g, 65%) was obtained as a yellow oil and used in the next step without further purification.

*Step 5, synthesis of (E)-methyl 4-((1,4-dimethylpiperazin-2-ylidene)amino)-3-(phenylcarbamoyl)benzoate (**68**)*. Method A as given for **45**. White solid (81 mg, 73%), mp 154-

158 °C (decomp.). ^{1}H NMR (400 MHz, $CDCl_3$) δ 10.91 (s, 1H), 8.93 (d, *J* = 2.2 Hz, 1H), 8.00 (dd, *J* = 8.3, 2.2 Hz, 1H), 7.67–7.62 (m, 2H), 7.38–7.32 (m, 2H), 7.13–7.07 (m, 1H), 6.77 (d, *J* = 8.3 Hz, 1H), 3.91 (s, 3H), 3.42 (t, *J* = 5.6 Hz, 2H), 3.26 (s, 3H), 3.09 (s, 2H), 2.65 (t, *J* = 5.6 Hz, 2H), 2.22 (s, 3H). ^{13}C NMR (126 MHz, $CDCl_3$) δ 166.9, 164.1, 156.1, 152.4, 138.8, 133.5, 132.8, 129.2, 125.8, 124.7, 124.0, 123.5, 120.3, 55.2, 52.1, 49.8, 45.5, 36.9. LC-MS: ^{t}R = 3.15 min, purity = 100%. HRMS (*m*/*z*): calcd for $C_{21}H_{25}N_4O_3$ $(M + H)^+$ 381.1921; found 381.1927.

Biology.

CPE-based Antiviral Assay. VEEV strains of TC-83, V3526 and TrD were amplified in BHK-21 cells. Anti-VEEV activity and cytotoxicity of compound was measured as described elsewhere.[27] Briefly, for a dose response study, test compounds were solubilized in DMSO at 20 mM first and then diluted further in DMSO by a two-fold serial dilution of 8-points. Compounds were diluted in cell growth media (EMEM with 10% FBS) then added to white cell plates in which Vero76 cells were grown overnight (seeding density of 12,000 cells/well in a volume of 45 µL). After a one-hour incubation, the cells were challenged with 600 plaque forming unit of virus per well. The cells were incubated for two days then cell viability was measured with 90 µL per well of CellTiter-Glo reagent (Promega). For cytotoxicity, cell media was used in place of virus and incubated for three days. Experiments were done in triplicate for efficacy test and duplicate for cytotoxicity test. For EC_{50} or CC_{50} calculation, relative cell viability compared to the non-infected cells controls was plotted using XLfit (IBDS) and EC_{50}s and CC_{50} were calculated using 4 Parameter Logistic Model or Sigmoidal Dose-Response Model.

Titer Reduction Assay. A microplaque assay was used.[27] Vero 76 cells grown in 6-well plates were infected with virus at an MOI of 0.05 and incubated in culture media with or without

compounds. At 40 hours post-infection, the titer of progeny virus in the media was measured as follows. Supernates from the 6 well plate from each treatment were diluted in DMEM supplemented with 5% FBS using a liquid handler, epMotion 5070 CB (Eppendorf Inc.). Vero 76 cells grown overnight in 96-well plates were infected with 25 μL of the serially diluted samples. The plates were incubated for 1 hour at 37 °C, 5% CO_2. Wells were rinsed with 100 μL of PBS and replenished with DMEM supplemented with 0.75% methylcellulose and 10% FBS and incubated at 37 °C, 5% CO_2 for three days. The microplaques were visualized by staining with 0.2% crystal violet in 4% paraformaldehyde and 20% ethanol.

***In Vivo* Antiviral Efficacy Studies**. Twenty-one C3H/HeN mice in the 5-6 week-old range were obtained from Charles River Laboratories (Wilmington, MA) and randomly assigned and evenly distributed to one of 3 treatment groups: Group 1 - vehicle control (no virus or compound treatment); Group 2 - VEEV only (no compound treatment); Group 3 - VEEV + compound treatment (5 mg/kg/day of compound **45**). Mice were dosed IP twice per day with vehicle only (1% carboxymethlycellulose, 200 μL, Group 1) or compound **45** formulated in 1% carboxymethlycellulose (2.5 mg/kg for each dose given twice a day, 200 μL each dose, Group 3). Treatments were administered for four days, beginning 4 hours prior to virus challenge for Group 3 (Day-0 to Day-3). Mice in groups 2 and 3 were infected intranasally with 10 times the LD_{50} of TC-83 (Day-0, virus diluted in 50 μL of PBS). For the Group 1 mice (vehicle control), PBS was used in place of virus. Mice were weighed from D0-D21 and checked twice a day for mortality and morbidity. The median time-to-death for the group challenged with VEEV was 8 days. P values were generated from comparisons of survival data using the Log-Rank (Mantel-Cox) test using Prism 6 (Graph Pad Software, Inc).

ASSOCIATED CONTENT

Analytical characterization and experimental details for synthesized intermediates, *in vitro* and *in vivo* pharmacology assay protocols, Eurofins Panlabs® Hit LeadProfiling data for compound **45**. This material is available free of charge via the Internet at http://pubs.acs.org.

AUTHOR INFORMATION

Corresponding Author

*E-mail: jengolden@ku.edu. Phone: (785) 864-6114 Fax: (785)-864-8179

NOTES

The authors declare no competing financial interest.

ACKNOWLEDGMENTS

The authors gratefully acknowledge funding from the following sources. Chemistry efforts at the University of Kansas Specialized Chemistry Center and pharmacokinetic analyses were supported by NIH U54HG005031 to J. Aubé. Support for the University of Kansas NMR instrumentation was provided by NIH Shared Instrumentation Grant number S10RR024664 and NSF Major Research Instrumentation Grant number 0320648. High throughput screening performed at the Southern Research Specialized Biocontainment Screening Center was supported by grant NIH U54HG005034-01, and D.-H. Chung acknowledges support from grant number R03 MH087448-01A1. *In vitro* ADME and *in vivo* DMPK studies performed at the *Conrad Prebys* Center for Chemical Genomics at the Sanford Burnham Medical Research Institute were supported by grant NIH U54 HG00503. The authors also wish to thank Daniel

Cremer for his support of the animal studies at the University of Louisville, Mr. Patrick Porubsky at the University of Kansas SCC for chemical and aqueous stability experiments, and Ms. Arianna Mangravita-Novo at the *Conrad Prebys* Sanford Burnham Medical Research Institute for performing *in vitro* ADME assessments.

ABBREVIATIONS USED

BBB, blood-brain barrier; cLogP, calculated partitian coefficient of a compound in octanol:water; CNS, central nervous system; CPE, cytopathic effect; DMEM, Dulbecco's modified Eagle's medium; EMEM, Eagle's Minimum Essential Medium; FBS, fetal bovine serum; HTS, high throughput screen; IP, intraperitoneal; MLPCN, Molecular Libraries Probe Production Centers Network; MWI, microwave irradiation; PBS, phosphate buffered saline; tPSA, topological polar surface area; TrD, Trinidad Donkey strain; VEEV, Venezuelan Equine Encephalitis Virus.

REFERENCES

(1) Johnston, R. E.; Peters, C. J. Alphaviruses. In *Fields Virology*, *3rd edition*; Fields, B. N.; Knipe, D. M.; Howley, P. M.; Chanock, R. M.; Melnick, J. L.; Monath, T. P.; Roizman, B.; Straus, S. E., Eds. Lippincott-Raven: Philadelphia, PA, 1996; pp 858-898.

(2) Calisher, C. H. Medically important arboviruses of the United States and Canada. *Clin. Microbiol. Rev.* **1994,** *7*, 89-116.

(3) Schmaljohn, A.L.; McClain, D. Alphaviruses (togaviridae) and flaviviruses (flaviviridae). In *Medical Microbiology, 4th edition.* Baron, S., Ed. National Institutes of Health: http://www.ncbi.nlm.nih.gov/books/NBK7633/, 1996.

(4) Nagata, L. P.; Wong, J. P.; Hu, W.-g.; Wu, J. Q. Vaccines and therapeutics for the encephalitic alphaviruses. *Future Virol.* **2013,** *8,* 661-674.

(5) Gubler, D. J. The global emergence/resurgence of arboviral diseases as public health problems. *Arch. Med. Res.* **2002,** *33*, 330-342.

(6) Sidwell, R. W.; Smee, D. F. Viruses of the bunya-and togaviridae families: potential as bioterrorism agents and means of control. *Antiviral Res.* **2003,** *57*, 101-111.

(7) Peng, W.; Peltier, D. C.; Larsen, M. J.; Kirchhoff, P. D.; Larsen, S. D.; Neubig, R. R.; Miller, D. J. Identification of thieno[3,2-b]pyrrole derivatives as novel small molecule inhibitors of neurotropic alphaviruses. *J. Infect. Dis.* **2009,** *199*, 950-957.

(8) Smith, J. F.; Davis, K.; Hart, M. K.; Ludwig, G. M.; McClain, D. J.; Parker, M. D. Viral Encephalitides. In *Medical aspects of chemical and biological warfare*, Sidwell, R. V.; Takafuji, E. T.; Franz, D. R., Eds. http://www.cs.amedd.army.mil/borden/Portlet.aspx?ID=bddf382f-3ca0-44ba-bd67-fdc48bfa03de, 1997; pp 561-589.

(9) Weaver, S. C.; Barrett, A. D. Transmission cycles, host range, evolution and emergence of arboviral disease. *Nat. Rev. Microbiol.* **2004,** *2*, 789-801.

(10) Iowa State University, College of Veterinary Medicine. Eastern equine encephalomyelitis, western equine encephalomyelitis and Venezuelan equine encephalomyelitis. http://www.cfsph.iastate.edu/Factsheets/pdfs/easter_wester_venezuelan_equine_encephalomyelitis.pdf, 2008; pp 1-9.

(11) Zacks, M. A.; Paessler, S. Encephalitic alphaviruses. *Vet. Microbiol.* **2010,** *140*, 281-286.

(12) Atasheva, S.; Garmashova, N.; Frolov, I.; Frolova, E. Venezuelan equine encephalitis virus capsid protein inhibits nuclear import in Mammalian but not in mosquito cells. *J. Virol.* **2008,** *82*, 4028-4041.

(13) Ehrenkrantz, N. J.; Ventura, A. K. Venezuelan equine encephalitis virus infection in man *Annu. Rev. Med.* **1974,** *25*, 9-14.

(14) McKinney, R. W.; Berge, T. O.; Sawyer, W. D.; Tigertt, W. D.; D., C. Use of an attenuated strain of Venezuelan equine encephalomyelitis virus for immunization in man. *Am. J. Trop. Med. Hyg.* **1963,** *12*, 597-603.

(15) Cole, F. E.; May, S. W.; Eddy, G. A. Inactivated Venezuelan equine encephalomyelitis vaccine prepared from attenuated (TC-83 Strain) virus. *Appl. Microbiol.* **1974,** *27*, 150-153.

(16) McKinney, R. W. Inactivated and live VEE vaccines – a review; Proceedings of the workshop symposium on Venezuelan Equine Encephalitis. *Sci. Publ. - Pan Am. Health Organ.* **1972,** *243*, 369-389.

(17) Edelman, R.; Ascher, M. S.; Oster, C. N.; Ramsurg, H. H.; Cole, F. E.; Eddy, G. A. Evaluation in humans of a new, inactivated vaccine for Venezuelan equine encephalitis virus (C84). *J. Infect. Disease* **1979,** *140*, 708–715.

(18) Davis, N. L.; Brown, K. W.; Greenwald, G. F.; Zajac, A. J.; Zacny, V. L.; Smith, J. F.; Johnston, R. E. Attenuated mutants of Venezuelan equine encephalitis virus containing lethal mutations in the PE2 cleavage signal combined with a second-site suppressor mutation in E1. *Virology* **1995,** *212*, 102-110.

(19) Holley, H.; Fine, D.; Terpening, S.; Mallory, R.; Main, C.; Snow, D.; Helber, S. In *Safety of an Attenuated Venezuelan equine encephalitis virus (VEEV) vaccine in humans.* Presented at the 48th Annual ICAAC/IDSA meeting, Washington, DC, October 25th, 2008.

(20) Julander, J. G.; Bowen, R. A.; Rao, J. R.; Day, C.; Shafer, K.; Smee, D. F.; Morrey, J. D.; Chu, C. K. Treatment of Venezuelan equine encephalitis virus infection with (-)-carbodine. *Antiviral Res.* **2008,** *80*, 309-315.

(21) Markland, W.; McQuaid, T. J.; Jain, J.; Kwong, A. D. Broad-spectrum antiviral activity of the IMP dehydrogenase inhibitor VX-497: a comparison with ribavirin and demonstration of antiviral additivity with alpha interferon. *Antimicrob. Agents Chemother.* **2000,** *44*, 859-866.

(22) Selvam, P.; Vijayalakshimi, P.; Smee, D. F.; Gowen, B. B.; Julander, J. G.; Day, C. W.; Barnard, D. L. Novel 3-sulphonamido-quinazolin-4(3H)-one derivatives: microwave-assisted synthesis and evaluation of antiviral activities against respiratory and biodefense viruses. *Antivir. Chem. Chemother.* **2007,** *18*, 301-305.

(23) Kehn-Hall, K.; Narayanan, A.; Lundberg, L.; Sampey, G.; Pinkham, C.; Guendel, I.; Van Duyne, R.; Senina, S.; Schultz, K. L.; Stavale, E.; Aman, M. J.; Bailey, C.; Kashanchi, F. Modulation of GSK-3β activity in Venezuelan equine encephalitis virus infection. *PLoS One* **2012,** *7*, e34761.

(24) https://mli.nih.gov/mli/mlpcn/

(25) PubChem Summary AID 588723

(26) Chung, D.-H.; Schroeder, C. E.; Sotsky, J.; Yao, T.; Roy, S.; Smith, R. A.; Tower, N. A.; Noah, J. W.; McKellip, S.; Sosa, M.; Rasmussen, L.; White, E. L.; Aubé, J.; Golden, J. E. *ML336: Development of quinazolinone-based inhibitors against Venezuelan equine encephalitis virus (VEEV)*; National Institutes of Health: NIH Bookshelf, 2012.

(27) Chung, D.-H.; Jonsson, C. B.; Tower, N. A.; Chu, Y.-K.; Sahin, E.; Golden, J. E.; Noah, J. W.; Schroeder, C. E.; Sotsky, J. B.; Sosa, M. I.; Cramer, D. E.; McKellip, S. N.; Rasmussen, L.; White, E. L.; Schmaljohn, C. S.; Julander, J. G.; Smith, J. M.; Filone, C. M.; Connor, J. H.; Sakurai, Y.; Davey, R. A. Discovery of a novel compound with anti-Venezuelan equine encephalitis virus activity that targets the nonstructural protein 2. *PLoS Pathog.* **2014,** *10*, e1004213.

(28) Promiscuity of hit compounds was defined by the number of unique assays that the compound was found to be active in divided by the number of unique assays the compound was tested in. A hit rate of less than 5% was desirable.

(29) Griffin, D. E. Viral Encephalomyelitis. *PLoS Pathog.* **2011,** *7*, e1002004.

(30) Pajouhesh, H.; Lenz, G. R. Medicinal chemical properties of successful central nervous system drugs. *NeuroRx* **2005,** *2*, 541–553.

(31) Ghose, A. K.; Herbertz, T.; Hudkins, R. L.; Dorsey, B. D.; Mallamo, J. P. Knowledge-based, central nervous system (CNS) lead selection and lead optimization for CNS drug discovery. *ACS Chem. Neurosci.* **2012,** *3*, 50-68.

(32) Intermediate **3** was generally obtained from the reaction; however, in some cases, we did obtain 2-(chloromethyl)benzoxazinone as the literature method described. When used as a substrate in the next reaction, either intermediate was efficiently converted to the desired chloromethylquinazolinone **4**.

(33) Stockwell, B. Compounds and compositions that cause non-apoptotic cell death and uses thereof. WO 2009108384A2.

(34) Acharyulu, P. V. R.; Dubey, P. K.; Reddy, P. V. V. P.; Suresh, T. Synthesis of Novel New 2-(2-(4-((3,4-Dihydro-4-oxo-3-aryl quinazolin-2-yl)methyl)piperazin-1-yl)acetoyloxy)-2-phenyl Acetic Acid Esters. *Synth. Commun.* **2009,** *39*, 3217-3231.

(35) Schroeder, C. E.; Yao, T.; Neuenswander, S. A.; Aubé, J.; Golden, J. E. *Unpublished results*.

(36) Hopkins, A. L.; Groom, C. R.; Alex, A. Ligand efficiency: a useful metric for lead selection. *Drug Discov. Today* **2004,** *9*, 430-431.

(37) Leeson, P. D.; Springthorpe, B. The influence of drug-like concepts on decision-making in medicinal chemistry. *Nat. Rev. Drug Discov.* **2007,** *6*, 881-890.

(38) Data obtained from Eurofins PanLabs (formerly Ricerca).

(39) Full panel inhibition data for compound **45** is supplied in the supplemental material.

(40) McAnally, D.; Vicchiarelli, M.; Siddiquee, K.; Smith, L. H. In vivo rapid assessment of compound exposure (RACE) for profiling the pharmacokinetics of novel chemical probes. *Curr. Protoc. Chem. Biol.* **2012,** *4*, 299-309.

(41) See supplemental Figure 3 for study design.

(42) Rich, J.T.; Neely, J.G.; Paniello, R.C.; Voelker, C.C.J.; Nussenbaum, B.; Wang, E.W. A practical guide to understanding Kaplan-Meier curves. *Otolaryngol. Head Neck Surg.* **2010,** *143,* 331-336.

(43) Shin, G.; Yost, S. A.; Miller, M. T.; Elrod, E. J.; Grakoui, A.; Marcotrigiano, J. Structural and functional insights into alphavirus polyprotein processing and pathogenesis. *Proc. Natl. Acad. Sci. U. S. A.* **2012,** *109*, 16534-16539.

(44) The mutant viruses were discovered by passing TC-83 in the presence of the hit compound, **1**. At passage 4, viruses that were resistant to the compound began to emerge. Studies of six resistant clones showed that their maximum virus titers were ~ 10-fold lower compared to the parental strain. This may indicate that the resistant viruses were less fitted forms compared to the parental strain (see reference 27, this paper). Currently studies to characterize the mutant viruses are in progress.

Table of Contents Graphic